universität wien

DIPLOMARBEIT

Titel der Diplomarbeit

Lentivirus Vector-Mediated Expression of Fluorescent Proteins in Human Melanoma Cell Lines and their Characterisation for *In Vivo* Visualisation of Tumour Growth

Verfasserin

Michaela Fischer

angestrebter akademischer Grad

Magistra der Naturwissenschaften (Mag.rer.nat.)

Wien, 2013

Studienkennzahl lt. Studienblatt:	A 490
Studienrichtung lt. Studienblatt:	Diplomstudium Molekulare Biologie
Betreuer:	Univ.-Prof. Mag. Dr. Pavel Kovarik

This diploma thesis was carried out under the supervision of O.Univ.-Prof. Dr.med.vet. Gottfried Brem at the Christian Doppler Laboratory for Innovative Immunotherapy at the University of Veterinary Medicine in Vienna.

ACKNOWLEDGEMENTS

I am grateful for those who participated in making my thesis possible. Special thanks go to my supervisor Juraj Hlavaty, PhD. who has always supported and encouraged me during my work.

I also thank Univ.-Prof. Mag. Dr. Pavel Kovarik for his offer to be my supervising tutor at the University of Vienna.

Special thanks go to my colleagues at the Institute of Virology and at the Christian Doppler Laboratory for Innovative Immunotherapy at the University of Veterinary Medicine in Vienna for their help, whenever I have needed it. I especially want to mention Mag. Martin Kraase who has always been available for informative discussions. Additionally, I thank Mag. Katrin Spiesberger for introducing me into the topic of killing assays and also Tobias Käser, PhD. for cell sorting. Thanks to Mag. Karina Scherrer for driving me to work - without her I would have been stuck on the train every morning.

I owe it to Dr. Dieter Fink; he and his plasmids made my work possible in the first place.

Last but not least I want to dedicate a special thank to my parents and to all the people I consider my family for their patience and personal support throughout my entire studies.

ABSTRACT

Within the group of skin cancer, malignant melanomas are the cause for about 75 % of deaths. Therefore, it is of high importance to test new therapeutic approaches in relevant *in vitro* experiments as well as in *in vivo* model systems. In recent years antibody-based immunotherapy has made great progress in the fight against malignancies. One promising antibody is the recombinant bispecific single-chain antibody r28M, which is directed against the Chondroitin sulfate proteoglycan 4 (CSPG4) on several types of tumour cells, including melanoma and glioblastoma cells, as well as the co-stimulatory CD28 antigen on human T-cells. Thus, r28M is able to induce activation of human T-cells without additionally signalling via the TCR/CD3 complex, which results in an effective killing of the tumour cells. To visualise tumours and the therapeutic effect of the r28M antibody on tumour cells in mice, genes for red and far-red fluorescence proteins can be stably transduced into these cells via lentiviral vectors.

The aim of this thesis was the generation and characterisation of different melanoma cell lines transduced with the genes for the fluorescence proteins mCherry and mKate2. Therefore, HIV-based lentiviral vectors pseudotyped with the VSV-G envelope were produced via calcium-phosphate transfection and used for infections of the melanoma cell lines A-375, SK-MEL-28 and IPC-298. In order to obtain populations of RFP-expressing cells, transduced cells were selected by blasticidin only or by blasticidin treatment followed by FACS-sorting. These cells were then studied for transduction stability and strength of the emitted fluorescence signal by flow cytometry. To exclude differences in growth behaviour between parental and transduced melanoma cells, growth curve analysis and doubling time calculations were carried out. After confirming the presence of the CSPG4 antigen on the melanoma cells by flow cytometry as well as the relative amount of CSPG4-expression by Western blotting, the r28M antibody was tested for its ability to induce killing of the transduced tumour cells *in vitro*. Subsequently, *mCherry*- and *mKate2*-transduced A-375 cells were injected subcutaneously into nude mice to visualise the resulting tumours via the IVIS 50 (Xenogen *in vivo* Imaging System). To establish a brain metastasis model the A-375 and SK-MEL-

28 cells both transduced with the gene for mCherry were injected directly into the brains of NSG mice, whereupon the emerged tumours could also be visualised non-invasively via the IVIS.

We could successfully generate *mCherry*- and *mKate2*-transduced A-375, SK-MEL-28 and IPC-298 cells with stable transduction rates and growth behaviour comparable to those of the parental cells. We found the target antigen CSPG4 to be present on almost all investigated melanoma cells. In addition, we showed similar amount of CSPG4-expression between parental and transduced cells, whereupon the A-375 cell line revealed to be killed most effectively by the PBMCs, when the dimeric form of the r28M antibody was applied *in vitro*. The tumours emerged by subcutaneous injection of the *mCherry*- or *mKate2*-transduced A-375 cells into immune-deficient mice were detectable via IVIS. Furthermore, the tumours in the brains of NSG mice could be monitored through skull and skin.

Thus, we could prove that virus infection and expression of the red fluorescence proteins neither altered the growth behaviour of the transduced cells, nor the expression of the CSPG4 antigen. Moreover, the tumours that had developed after injection of transduced melanoma cells into immune-deficient mice were detectable non-invasively.

The approaches described in this thesis will be used as a base for non-invasive visualisation of tumours and their response to medical substances in pre-clinical animal experiments in the future.

ZUSAMMENFASSUNG

Maligne Melanome sind die Ursache für ungefähr 75 % der Todesfälle innerhalb der Gruppe des Hautkrebs. Daher ist es sehr wichtig dafür neue therapeutische Ansätze in entsprechenden *in vitro* Experimenten und *in vivo* Modellsystemen zu testen. In den vergangenen Jahren hat die antikörper-basierte Immuntherapie große Fortschritte im Kampf gegen maligne Tumore gemacht. Ein vielversprechender Antikörper ist der rekombinante bispezifische Einzelketten-Antikörper r28M, der sowohl gegen das Chondroitinsulfat-Proteoglycan 4 (CSPG4) auf verschiedenen Tumorzellen, darunter Melanom- und Glioblastomzellen, als auch gegen das co-stimulatorische CD28 Antigen auf humanen T-Zellen gerichtet ist. Daher kann der r28M Antikörper die Aktivierung von humanen T-Zellen ohne Signalisierung über den TCR/CD3 Komplex bewirken, was zum Absterben der Tumorzellen führt. Um Tumore und den möglichen Effekt des r28M Antikörpers auf diese in Mäusen sichtbar zu machen, können mittels lentiviraler Vektoren Gene für Fluoreszenzproteine mit Emissionsspektren in den roten und dunkelroten Wellenlängen in Tumorzellen transduziert werden.

Das Ziel dieser Arbeit war die Herstellung und Charakterisierung von verschiedenen, mit den Genen für die Fluoreszenzproteine mCherry und mKate2-transduzierten, Melanomzelllinien. Dafür wurden via Calcium-Phosphat-Präzipitation HIV-basierte lentivirale Vektoren, pseudotypisiert mit der VSV-G Hülle, produziert und diese für Infektionen der Melanomzelllinien A-375, SK-MEL-28 und IPC-298 benutzt. Um Populationen von RFP-expremierenden Zellen zu erhalten wurden die transduzierten Zellen entweder nur mittels Blasticidin oder mittels Blasticidin mit anschließender FACS-Sortierung selektiert. Diese Zellen wurden dann via Durchflusszytometrie auf Transduktionsstabilität und Stärke ihres emittierten Fluoreszenzsignals hin untersucht. Um Unterschiede im Wachstums-verhalten zwischen parentalen und transduzierten Melanomzellen auszuschließen, wurden Wachstumskurvenanalysen und Verdopplungszeitenberechnungen durchgeführt. Nachdem sowohl via Durchflusszytometrie die Präsenz des CSPG4 Antigens auf den Melanomzellen als auch mittels Western Blot die relative Menge der CSPG4-Expression herausgefunden wurden, wurde der r28M Antikörper auf

seine Fähigkeit hin getestet, die Zerstörung der transduzierten Tumorzellen *in vitro* auszulösen. Daraufhin wurden *mCherry*- und *mKate2*-transduzierte A-375 Zellen subcutan in haarlose Mäuse injiziert um die daraus resultierenden Tumore mittels dem IVIS 50 (Xenogen *in vivo* Imaging System) zu visualisieren. Um ein Metastasenmodel des Gehirns zu etablieren wurden die A-375 und SK-MEL-28 Zelllinien, beide mit dem Gen für mCherry transduziert, direkt in die Gehirne von NSG Mäusen injiziert und die daraus entstandenen Tumore via IVIS visualisiert.

Wir konnten *mCherry*- und *mKate2*- transduzierte A-375, SK-MEL-28 und IPC-298 Zellen erzeugen, die stabile Transduktionsraten und Wachstums-eigenschaften ähnlich zu denen der parentalen Zellen aufwiesen. Des Weiteren wiesen wir das Zielantigen CSPG4 auf nahezu allen untersuchten Melanomzellen nach. Zusätzlich zeigten wir vergleichbare Mengen an CSPG4-Expression zwischen parentalen und transduzierten Zellen, woraufhin die A-375 Zelllinie *in vitro* von den PBMCs am effektivsten zerstört wurde, wenn der r28M Antikörper in seiner dimeren Form zugegeben wurde. Die Tumore, die nach subcutaner Injektion der *mCherry*- oder *mKate2*-transduzierten A-375 Zellen gebildet wurden, konnten via IVIS in den immundefizienten Mäusen nachgewiesen werden. Auch die Gehirntumore der NSG Mäuse konnten durch Schädelknochen und Kopfhaut detektiert werden.

Wir konnten nachweisen, dass die Virusinfektion und die Expression der Fluoreszenzproteine weder das Wachstumsverhalten der transduzierten Zellen, noch deren CSPG4-Expression beeinflusste. Des Weiteren waren die Tumore nach Injektion der transduzierten Zellen in immundefiziente Mäusen nicht-invasiv detektierbar.

Die Vorgehensweisen, die in dieser Diplomarbeit beschrieben werden, werden in Zukunft als Basis für eine nicht-invasive Visualisierung von Tumoren und deren Ansprechen auf medizinische Substanzen in pre-klinischen Tierversuchen genutzt.

TABLE OF CONTENTS

1 INTRODUCTION

1.1 Cutaneous malignant melanoma

Malignant melanomas develop due to malignant transformations of melanocytes, which produce the dark pigment of the skin (melanin), but they can also be found in other organs such as the eye[1] or the gastrointestinal tract[2]. Although malignant melanomas account for only less than 5 % of all skin cancers[3], they are the cause for about 75 % of deaths within this group[4]. Moreover, the incidence rate of melanoma has shown a continuing increase of new cases among Caucasian populations worldwide in the last decades.[5]

1.1.1 Melanoma progression

In response to cell damaging agents (e.g. UV radiation) aberrant proliferation of melanocytes occurs, which causes the formation of benign or dysplastic nevi.[6] When cell senescence has been overcome, the dysplastic nevus can enter the radial growth phase (RGP) of primary melanoma, which is characterized by a low invasive potential.[6,7] Those cells also can gain the ability to enter the vertical growth phase (VGP) of primary melanoma when they invade dermis and metastasise.[6,7]

1.1.2 Risk factors contributing to development of malignant melanoma

Risk factors for the development of melanoma and its different specificities are diverse. In general, cancer arises due to DNA-damage inside cells, which can be caused by inherited genetic mutations or accumulation of new mutations over a person's lifetime. Thereby environmental factors are essential for tumour development. Moreover, epigenetic events, such as DNA methylation, play an important role in the initiation and progression of melanoma.[112]

1.2 Conventional therapies for malignant melanoma

In contrast to the highly curable early stage, the prognosis for melanoma patients with advanced stage tumours is sinister.[8,9] Melanomas tend to become

resistant to anti-cancer strategies used in clinics, including radio- and chemotherapy.[10,11] Immunotherapy with interleukin-2 (IL-2) has shown to have the ability for a complete and long-lasting remission from malignant melanoma, but was restricted to only a low number of patients with a response rate of 15 %.[12] Another immunotherapy agent is IFN-α, which is the only FDA approved adjuvant therapy for surgically resected melanoma of a tumour thickness of ≥ 4 mm.[13] The latest systematic review of 2012 concluded that patients with high-risk resected primary melanoma do not benefit from adjuvant therapy with interferon in long-term overall survival (OS).[14] Nevertheless, the authors illustrated numbers of significant benefit in disease-free survival (DFS) for high-dose interferon or pegylated interferon treatment.[14] The Federal Drug Administration (FDA) approved standard therapy for the treatment of metastatic melanoma has been the chemotherapeutic agent dacarbazine. Nevertheless, the response rates have turned out to be less than 10% in recently evaluated randomized controlled trials.[13] Vemurafenib was approved by the FDA in 2011 after a study had shown advantage in progression free survival (PFS) and OS when compared to dacarbazine.[15] Nevertheless, none of these strategies have shown a clear survival impact[12-14] which points out the urgency for the development of novel and improved therapeutic approaches for the fight against malignant melanoma.

1.2.1 Antibody-based therapies

Antibody-based therapy against melanomas has made great progress in the last few years and is now one of the most important treatment strategies against these malignancies. One of these antibodies is ipilimumab which was approved by the FDA for therapy of unresectable or late-state metastatic melanoma in 2011.[16] This human monoclonal antibody blocks the cytotoxic *T-lymphocyte–associated antigen 4* (*CTLA-4*) inhibitory signal to promote antitumour immunity.[17] A phase III study from 2010 revealed improved OS in patients with previously treated or unresectable metastatic melanoma when ipilimumab was administered as monotherapy or in combination with the glycoprotein 100 (gp100) cancer vaccine.[18] In contrast to monotherapy, combinations of diverse drugs have shown to be more beneficial. For example, a phase III first-line trial, carried out in 2011,

revealed significant improvement in OS among patients suffering from metastatic melanoma treated with ipilimumab plus dacarbazine compared to dacarbazine plus placebo.[19]

1.3 Bispecific antibodies

Bispecific antibodies (bsAb) combine two different antigenic specificities whereby they are able to redirect effector cells (like T-cells or NK-cells) towards therapeutic targets.[20] To mediate this redirected lysis, it is essential that the bsAb binds the target cell directly to a triggering molecule on the effector cell.[21]

Numerous strategies for the preparation of bsAbs (for example, by chemically linking two different monoclonal antibodies or by fusing of two hybridoma cell lines[22]) are available. Moreover, variations of these antibodies were developed by genetic engineering approaches. Bispecific antibodies were produced, in which the heavy-chain V-region (V_H) and light-chain V-region (V_L) domains bind non-covalently to form an 'F_v'.[21] Also single-chain (sc) F_vs were generated by joining the carboxyl terminus of one V-domain to the amino terminus of the other.[21] The linkage of two scF_vs can give a single-chain bispecific antibody (sc-bsAb) that binds both antigens, whereupon redirection of lysis occurs *in vitro*[23] as well as *in vivo*[24].

The biological responses induced by bsAbs reach from induction of cytotoxicity, phagocytosis and antigen-presentation over cytokine-release by activated effector cells.[20]

1.3.1 Bispecific single-chain antibody r28M

As mentioned above, standard therapy approaches have not fulfilled the expectations in the treatment of malignant melanoma. There is still an urgent need to develop a targeted therapy against the progression of the malignancy.

The r28M antibody is a recombinant bispecific single-chain antibody, which is on one hand directed against a melanoma-associated membrane-bound proteoglycan, named Chondroitin sulfate proteoglycan 4 (CSPG4) and on the other hand against the co-stimulatory CD28 antigen on human T-cells.[25] The schematic structure of r28M is shown in Figure 1.[26] Under physiological conditions

T-cell activation occurs after stimulation of the TCR/CD3 complex as well as of receptors for co-stimulatory signals, out of which the CD28 molecule and its ligands, CD80 (B7-1) and CD86 (B7-2) on antigen presenting cells (APCs), represent the most important ones.[26] The r28M antibody, however, induces remarkably efficient tumour cell-restricted T-cell activation via the CD28 molecule without a primary signal via the TCR/CD3 complex, when bound to tumour cells, which results in efficient tumour-cell killing *in vitro* as well as in a xenogeneic mouse glioblastoma model *in vivo*.[25,26] It was shown that the treatment of those mice with r28M and PBMCs resulted in a clear delay of tumour growth.[26] In addition, T-cell activation depends on the presence of CSPG4-positive tumour cells.[26] Moreover, the r28M antibody reveals a relatively long serum half-life and can be obtained in high concentrations from transgenic animals[26], whereupon the r28M protein produced in transgenic cows and rabbits was shown to retain its biological activity.[27]

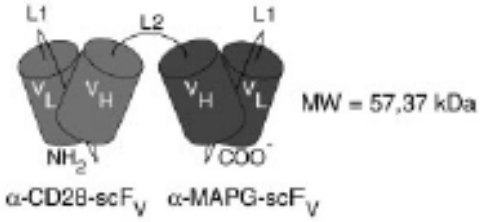

Figure 1. Schematic r28M structure.[26] The r28M antibody consists of two monospecific single-chain F_V fragments with a glycin serin linker (L1) between their V_H/V_L regions connected by a second linker (L2) to form a bispecific single-chain molecule with a calculated molecular weight of 57.37 kDa.

It was suggested that tumour cell killing facilitated by the supra-agonistic activity of the r28M antibody had occurred due to homodimerization as it had been indicated by gel filtration analysis.[28] When the antibody had been further examined it was shown that the supra-agonistic activity descended mainly from spontaneously formed, stable dimeric versions of the molecule.[28] Dimerization results in two binding sites for both, CD28 and the tumour antigen[29] which makes the antibody more effective in tumour cell killing. Moreover, it was found that the recombinant dimeric molecules induce T-cell activation comparable to the

stimulation with phytohaemagglutinin (PHA) at a low concentration of about 10 ng per ml.[29] In contrast, the monomeric r28M molecules reveal activation of T-cells only at high concentrations, starting at 1000 ng per ml.[29] When SK-MEL-63 cells were incubated together with PBMCs and the r28M antibody in its dimeric form, up to 70 % of the tumour cells were killed, whereas the killing effect was significantly weaker when the monomer was applied.[29]

In 2008 Otz et al. were able to reproduce the supra-agonistic CD28 stimulation, as caused by the r28M antibody, by exchanging the CSPG4-targeting part of r28M with a single-chain antibody directed to the B-cell associated antigen CD20, thus showing that the T-cells were able to destroy lymphoma target cells.[28]

In 2006 a monospecific and super-agonistic CD28 antibody termed TGN1412 induced severe cytokine release syndrome when injected into some patients.[30] However, there are differences between TGN1412 and the bispecific antibody r28M: In contrast to the activity of TGN1412, supra-agonistic CD28 stimulation by r28M is CSPG4-positive target-cell restricted[26], and this may avoid these kinds of side-effects.[31]

1.4 Chondroitin sulfate proteoglycan 4

The recombinant bispecific single-chain antibody r28M is targeted against the chondroitin sulfate proteoglycan 4 (CSPG4), which is also known as rat ortholog nerve/glial antigen 2 (NG2) or high molecular weight-melanoma associated antigen (HMW-MAA).[25,32] It is a cell surface type 1 transmembrane protein that was originally identified as a tumour antigen highly expressed on melanoma cells.[33] CSPG4 is present on about 85% of melanomas[34], but can also be detected in several other types of tumour cells like oligodendrocytomas, gliomas, neuroblastomas, triple-negative breast carcinomas, squamous cell carcinomas of the head and neck and renal cell carcinomas.[32]

Throughout development CSPG4 can be found in several types of normal tissues including angiogenesis associated pericytes[35,36], several pluripotent progenitor cell populations[37], mesenchymal cells of the bone marrow, and smooth muscle cells[32]. Moreover, it was shown that CSPG4-positive cells generate oligodendrocytes, protoplasmic astrocytes and neurons *in vivo*.[38]

With its multi-functionality CSPG4 plays an important role in melanoma progression by influencing various oncogenic signalling pathways that are altered during multiple stages of malignant progression.[32] Thus, CSPG4 can reinforce tumour cell characteristics including growth, motility, angiogenesis, survival and chemoresistance.[32]

1.4.1 CSPG4 signalling in malignant progression

During multiple stages of malignant progression the expression of this highly immunogenic tumour antigen enhances growth, survival, migration, invasion, protease activation, and epithelial to mesenchymal transition (EMT) through high-level activation of different signalling pathways.[39] These pathways can be divided into two main types: i) receptor tyrosine kinase (RTK) signalling through the mitogen-activated protein kinase (MAPK) cascade and ii) integrin signalling trough activation of focal adhesion kinase (FAK).[39] Price et al. created a schematic overview over the signalling pathways of CSPG4, which is presented in Figure 2.[32]

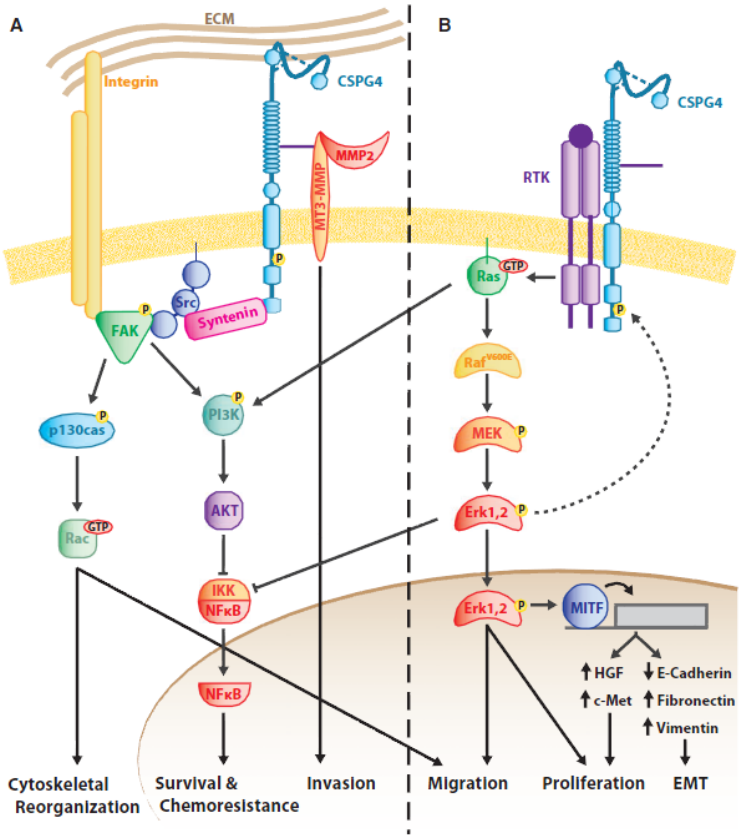

Figure 2. Signalling Pathways of CSPG4.[32] CSPG4 can activate **A.** integrin/focal adhesion kinase (FAK) and **B.** mitogen-activated protein kinase (MAPK) pathway signalling and is therefore promoter of tumour progression. **A.** Activation of FAK dependent pathways is done via interaction of CSPG4 with the scaffold protein syntenin, which results in Src-FAK complexing. FAK activation leads to the activation of different downstream signalling cascades, including the p130cas/Rac and the PI3K/AKT/NFκB cascade. This results in cytoskeletal reorganization, chemoresistance, and enhanced survival and migration. Local invasion of cancer cells is caused by activation of Matrix Metalloproteinases (MMPs). CSPG4 can also activate integrin-related signals and therefore also enhances survival. **B.** There are RTK-dependent and independent mechanisms through which CSPG4 promotes MAPK signalling. In the case of human melanomas, CSPG4 is likely to have an impact on activation of RTKs and therefore activates the ERK 1,2 pathways. $BRAF^{V600E}$ expression leads to steady activation of these RTKs. Melanocyte lineage-specific transcription factor (MITF), activated c-Met and other downstream oncogenic targets of the ERK 1,2 pathway are associated with proliferation and EMT. In addition, ERK 1,2 downstream of CSPG4 may cause cell survival and chemoresistance through the inhibiton of the I kappa B kinase (IKK).

1.4.2 CSPG4 as target in immunotherapy

In recent years, CSPG4 has been the target of choice for a number of immunotherapeutic approaches aimed at tumour progression delay with a minimum of side effects. These approaches include antibody therapy with anti-idiotype antibodies that lead to a significant increase in survival as well as with anti-anti-idiotopic antibodies that were able to induce HLA class I-restricted CSPG4-specific CTL.[32] Moreover, CSPG4 turned out to be an important therapeutic target when combined with inhibitors of oncogenic $BRAF^{V600E}$.[39] In 2010 Wang et al. demonstrated that an anti-CSPG4 monoclonal antibody leads to inhibition of growth and metastasis of human melanoma and basal breast tumour xenografts.[40] In another study from 2011 CSPG4 knockdown performed by intracerebral delivery of lentivirally encoded shRNAs targeting CSPG4 in patient glioblastoma xenografts as well as in subcutaneous A-375 melanomas reduced melanoma proliferation and increased apoptosis and necrosis.[41] Thus, targeting CSPG4 in heterogenous GBM xenografts significantly reduced tumour growth and angiogenesis and led to normalisation of vascular function.[41] Moreover, this vascular normalisation was followed by increased tumour invasion and decreased apoptosis and necrosis.[41]

Summarising, CSPG4 provides a suitable target for antibody-based therapy against melanomas and a wide range of other types of tumours.

1.5 Visualisation via red fluorescence proteins (RFPs)

For the visualisation of tumour cells *in vivo* it is helpful if they express appropriate reporters like fluorescent proteins or luciferase.

Bioluminescent imaging (BLI) with luciferase has shown to be suitable for quantification of tumour growth, gene expression and drug response.[42] Nevertheless, administration of luciferin via direct injection into the animals is necessary to generate the bioluminescence signal before images can be taken. Moreover the quality of this signal strongly depends on the efficiency of luciferin delivery into the organs of interest.[43] Thus, restricted delivery of luciferin into poorly perfused and hypoxic tumours may restrain light emission rates particularly

in the brain.[44,45] Another crucial disadvantage is the blue spectrum of the emitted signal, which has been indicated to be only sub-optimal for *in vivo* imaging.[46]

Therefore, the expression of red fluorescence proteins is often used to study cancer processes, including primary tumour growth, tumour cell motility and invasion, metastatic seeding and colonization, angiogenesis as well as the interaction between the tumour and its microenvironment.[47]

For deep imaging of animal tissues proteins with emission spectra in the red and far-red wavelengths offer the best choice.[48,49] In contrast to the green fluorescent protein (GFP), red-shifted fluorescent proteins provide better signal penetration through biological tissues.[35] Excitation at longer wavelength than those of GFP and yellow fluorescent protein (YFP) avoids generation of autofluorescence backgrounds derived from excitation of proteins with emission spectra in this wavelengths, like the flavin proteins or haemoglobin.[50,51] The excitation wavelengths for red fluorescent proteins range from about 550 to 650 nm, thus enabling real-time imaging without causing harm to the animals' tissues.[47] Moreover, RFPs are less sensitive to photodamage and thus can be used for cell visualisation over a longer time period, which is particularly important for real-time tracking of tumour growth and metastasis in the living animal.[52] They are also suitable for the use in two-colour, single-molecule imaging, because of their distinctness from GFPs and YFPs.[50] A study from 2003 showed that the tumour areas measured by RFP-imaging correlate with the volumes of resected pancreatic tumours.[53] Thus, whole-body RFP-imaging can be the method of choice for the quantification of tumour growth and metastasis.[53] Furthermore, the technique can be used for investigations of therapeutic anticancer treatments efficacy, for example of antimetastatic agents.[54]

1.5.1 mCherry and mKate2

Due to the advantages of red fluorescent proteins in the non-invasive visualisation of tumour cells *in vivo*, two different fluorescence proteins with their emission spectra in the red or far-red wavelengths were chosen for the intended monitoring of melanoma cells in immune-deficient mice.

The first is mCherry[55], which belongs to the new generation of red monomeric RFPs (mRFPs). The benefits in the use of mCherry with its excitation maximum at 587 nm and its emission maximum at 610 nm lie in brighter fluorescence and higher photostability compared to mRFP.[56] Moreover, mCherry matures more rapidly and shows a higher tolerance for N-terminal fusion proteins.[56] Although it belongs to the dimmest of the RFPs, mCherry could even be detected in live bacterial cells.[57] Due to its superior photostability and its relatively low molecular weight Shaner et al. claimed that mCherry is the best general-purpose red monomer compared to other RFPs of the mFruit series like tdTomato or mStrawberry.[58]

The second fluorescent protein chosen is mKate2[51] with an excitation and emission peaking at 588 and 633 nm. It is a monomeric far-red fluorescent protein generated through continued mutagenesis of its ancestor mKate, which was reported to reveal exceptional photostability.[49] mKate2 is three times brighter than mKate and shows excellent pH resistance and photostability.[51] Studies from 2009 revealed it as a suitable candidate for imaging applications in living animals, because of its low toxicity.[49]

In 2011 Verreault et al. successfully established glioblastoma cell lines expressing mCherry and mKate2 to follow progression and regression of orthotopic GBM tumours in living mice.[59] Moreover those cell lines enabled them to monitor the treatment of an antitumor drug.[59]

Therefore, mCherry and mKate2 are the tools of choice for the prospective non-invasive visualisation of tumour growth and the effect of the r28M antibody in immune-deficient mice.

1.6 Transduction via HIV-1-based vectors

For stable transduction of eukaryotic cells with genes for fluorescence proteins lentiviral vectors were preferred over other transfection methods. Viral transduction often results in higher transfection efficiency compared to those of non-viral delivery methods.[60] Moreover, viral transduction offers the ability to transduce even poorly transfectable cells without any cellular toxicity observed.[61] Lentiviral vectors in particular feature useful properties for gene delivery, including

stable vector integration into the host genome, the ability to infect dividing and also non-dividing cells, a broad tissue tropism, and relatively high safety in use due to diverse modifications of the viral genome.[62,63]

1.6.1 HIV-1 genome

The human immunodeficiency virus (HIV) represents one member of the genus *Lentivirus* and belongs to the family of *Retroviridae*. Lentiviruses are single-stranded, positive-sensed, enveloped RNA viruses and characterized by their use of viral reverse transcriptase (RT) and integrase (IN). A schematic drawing of the HIV-1 genome is shown in Figure 3.[64]

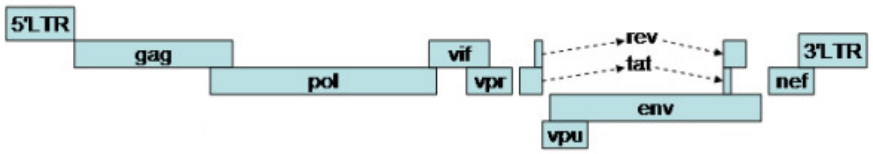

Figure 3. Schematic drawing of the HIV-1 genome (adapted).[64] The genome is approximately 9.8 kb long and harbours the main structural genes ga*g, pol* and *env* and the specific genes for the regulatory proteins Tat and Rev as well as for the accessory proteins Vif, Vpr, Vpu and Nef.

1.6.2 Four-plasmid vector system

Lentiviral vectors have successfully been used to transduce a number of cell types including neurons and haematopoietic stem cells.[65,66] Due to stable gene transduction, as facilitated by lentiviral vectors, *in vivo* monitoring or live imaging of cells is possible. Especially cancer cells that are stably transduced with reporter genes, can be monitored for their growth and metastasis *in vivo* by different means of methods like bioluminescence, fluorescence and positron emission tomography (PET) imaging.[67]

The most common lentiviral vectors/packaging constructs for transduction of foreign genetic material into host cells used nowadays have arisen from third generation lentiviral vectors, in which the viral genomes are splitted into multiple plasmids. To further enhance safety, the viral accessory proteins Tat, Vif, Vpr and Nef are deleted from the original plasmid.[62] These viral vectors are designed to be

Tat-independent with Rev situated on a separate plasmid.[62] Tat-independence is due to replacing the U3 promoter region of the 5'-LTR in the transfer vector with strong viral promoters like those from cytomegalovirus (CMV) or rous sarcoma virus (RSV).[64] Moreover the enhancer/promoter region of the 3'-LTR is removed, which provides self-inactivating (SIN) property.[62]

Schematic drawings of the virus vectors and the transfer vector used in this project are illustrated in Figure 4. The *gag* and *pol* genes are driven by a CMV promoter and located on the plasmid HIV-pLP1, which serves as the HIV-packaging construct. The *rev* gene is situated on the second plasmid HIV-pLP2 and driven by an RSV promoter. The retroviral Env glycoprotein is replaced by the viral attachment protein of VSV-G and placed on the third plasmid termed pHCMV-G. Pseudotyping of the vector with the VSV-G glycoprotein results in a vector that can infect also non-rodent mammalian cell types including human cells.[62] The transfer vectors harbour either the gene for mCherry or the gene for mKate2.

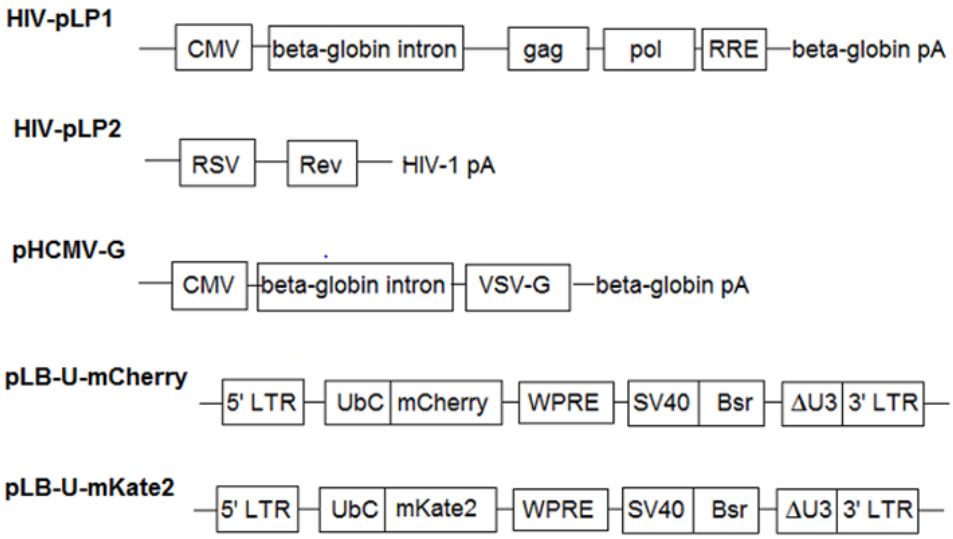

Figure 4. Lentiviral vector constructs. Together with the transfer vectors containing the genes for fluorescent proteins, they can generate a lentiviral vector of the third generation. The packaging construct HIV-pLP1 expresses the *gag* and *pol* genes from the CMV promoter and polyadenylation site of the human β-globin gene. All *tat* and *rev* exons have been deleted, and the viral sequences upstream the *gag* gene have been replaced. A nonoverlapping construct, HIV-pLP2, expresses the *rev* cDNA. Another construct, pHCMV-G, encodes a heterologous VSV envelope to pseudotype the vector. The transfer vector is containing the gene of interest and is driven by an UbiquitinC promoter.

1.7 Mouse Model of human metastasis

Human melanomas generally show strong tendencies to form metastases in brain, lung, liver and skin.[68] In about 60 to 80 % of patients with metastatic melanoma metastasis occurs in the brain, which is the major cause of death in these patients.[69] From presentation with brain metastases to death patients with single brain lesions show a median survival time of 5 months, whereas median survival is even 2 months less for patients showing multiple lesions[70]. This points out the importance of establishing *in vivo* models of melanoma metastasis in the brain.

As tumours, which emerged by subcutaneous injections of tumour cells, are not always able to develop brain metastasis in mice[71] these tumour cells can be injected directly into the brain. To study tumour characteristics mice of the NOD.Cg-Prkdc^{scid} Il2rg^{tm1Wjl}/SzJ (NSG) mouse strain are often used. They were developed in the Jackson Laboratory and are based on the inbred NOD mouse strain NOD/ShiLtJ.[72] They show reduced innate immunity including defective macrophage and defective dendritic cell activity.[72] They furthermore harbour an allele of the *Sirpa* gene that makes their bone marrow highly permissive to colonisation by human hematopoietic stem cells.[72] Another feature of the NSG strain is its Prkdc^{scid} mutation, which eliminates adaptive immunity.[72] Mice homozygous for this mutation show remarkably reduced numbers of mature B and T cells.[72] The presence of differentiated natural killer (NK) cells constituted a major obstacle for efficient engraftment of primary human cells. NSG mice have an Il2rg^{tm1Wjl} targeted mutation, which is a null mutation (knockout) in the gene for the interleukin 2 receptor gamma chain (IL2Rγ), resulting in defect differentiation and functioning of NK cells.[72]

Moreover, NSG mice provide the best hosts for human hematopoietic stem cells to produce humanized mice for vaccine models, since they are lacking immune cells including T, B, and especially NK cells.[72,73] Additionally, the Sirpa polymorphism inhibits the mouse macrophages from engulfing the human hematopoietic stem cells.[72] The *scid* mutation is suggested to improve engraftment of human hematopoietic stem cells in the bone marrow niche.[72] Besides, NSG

mice do not require irradiation before injection of the PBMCs to generate humanized mice.[72]

Under optimal conditions NSG mice can live for over 1.5 years, because they do not develop thymic lymphoma, which is the major cause of death within NOD scid mice.[72,74]

1.7.1. NSG-mice as melanoma model

Multiple applications of human immune system engrafted NSG mice are known, including studies of infectious diseases, cancer as well as testing new therapies against these afflictions.[75] They are further used to study cancer stem cells including melanoma and leukemia stem cells.[76]

NSG mice are reported to show rapid tumour engraftment in a melanoma model compared to *scid* and NOD-*scid* mice, in which melanoma metastases growth was delayed and variable.[73] They can further increase the detection of tumourigenic melanoma cells by several orders of magnitude.[77]

Moreover, they represent the basic mouse strain to generate humanized mice[74] for our prospective testing of the effects of the r28M antibody on the transduced melanoma cells *in vivo*. Thus, they were also taken to verify the tumourigenicity of the *mCherry*- or *mKate2*-transduced cells as well as to measure the RFP signal penetration through their skull and skin.

2 AIM OF THE THESIS

Since visualisation of fluorescence signal emitting tumours can be used to monitor tumour progression, this method offers the possibility to study the efficiency of the bispecific antibody r28M on tumour cells *in vivo*. In this thesis, the development and characterisation of the different melanoma cell lines A-375, SK-MEL-28 and IPC-298, expressing the fluorescent proteins mCherry or mKate2 for visualisation of tumours and their growth, is described.

In the first part of my studies I aimed at generating populations of melanoma cells stably expressing the respective fluorescent proteins by the means of lentiviral transduction.

The second part of my research addressed the question, whether or not the lentivirally transduced melanoma cells showed any changes in key characteristics important for prospective testing of the r28M antibody compared to their parental cells. To exclude possible differences in doubling times, growth curve analysis was performed. Moreover, similar expression of CSPG4, which is the target antigen for the r28M antibody, was verified. Further, r28M was tested for its ability to induce comparable killing of the parental as well as transduced tumour cells in *in vitro* cell viability assays.

To answer the question if the transduced cells kept their tumourigenicity as well as if the emerged tumours could be visualised non-invasively, chosen cell lines were injected into the brains of immune-deficient mice.

Since the mCherry- as well as the mKate2-expressing tumours were successfully visualised through skull and skin, the approach described in this thesis will provide the basis for prospective monitoring of the therapeutic effects of the r28M antibody in humanized mice.

3 MATERIALS

3.1 Transformation of bacteria and plasmid isolation

- NEB 5-alpha Competent *E.Coli* (High Efficiency) (New England Biolabs (NEB); # C2987H)
- DNA Plasmids HIV-pLP1 and HIV-pLP2 were a generous gift from Renata Stripecke, Department of Hematology, Hemostasiology, Oncology and Stem Cell Transplantation**,** Hannover Medical School, Germany.
- pLB-U-mCherry (Supplement 1) and pLB-U-mKate2 (Supplement 2) were a generous gift from Dieter Fink, Biomodels Austria, University of Veterinary Medicine, Vienna, Austria.
- pHCMV-G was a generous gift from Dorothee von Laer, Institute for Biomedical Research, Georg-Speyer-Haus, Frankfurt, Germany.
- LB medium: 10 g Tryptone (Sigma-Aldrich, # 16922)
  10 g Yeast Extract (Sigma-Aldrich, # 70161)
  10 g NaCl (Sigma, # S 3014)
  dissolved in 1 l $_{dd}H_2O$, adjusted to pH 7.0 and autoclaved
- LB – Agar: LB medium containing
  15 g/l agar (Sigma-Aldrich, # 05039) and
  0.1 µg/ml ampicillin (Sigma-Aldrich, # A5354)
- Qiagen Plasmid Maxi Kit (Qiagen, # 12163)
- Isopropanol (Merck, # 1.09634.1011)
- Ethanol (Merck Millipore, # 108543)
- NanoDrop 1000 Spectrophotometer

3.2 Restriction digestion and agarose gel electrophoresis

- Restriction enzymes (with optimal buffers; Thermo Scientific):
  - PstI (# ER0611)
  - EcoRI (# ER0271)
  - BamHI (# ER0051)
  - HindIII (# ER0501)

  - PvuII (# ER0631)
  - XbaI (# ER0681)
  - Bsp1407I (BsrGI) (# ER0931)
  - FastDigest SacI (# FD1134)
- PeqGOLD Universal-Agarose (Peqlab, # 35-1020)
- Gel apertures from Peqlab
- TAE buffer (50 x): 242 g Tris Base (Fisher Scientific, # BP152-500)
  57.1 ml Acetic Acid (Sigma-Aldrich, # 320099)
  100 ml 0.5 M EDTA (Life technologies; # AM9260G)
  dissolved in 1 l $_{dd}H_2O$
- DNA markers (GeneRuler, ready-to-use; Fermentas):
  - 1 kb DNA Ladder, 250-10,000 bp (# SM0314)
  - DNA Ladder Mix, 100- 10,000 bp (# SM0334)
  - 100 bp Plus DNA Ladder, 100-3000 bp (# SM0322)
- 6x Orange DNA Loading Dye (Fermentas, # R0631)
- Ethidium bromide (Merck, # 1116080030)

3.3 Cell Culture

3.3.1 Cells

- HEK-293T (ATCC, # CRL-1573)
- A-375 (CLS, # 300110)
- SK-MEL-28 (CLS, # 300337)
- IPC-298 (DSMZ, # ACC 251)
- PBMCs (freshly isolated from healthy volunteers by Spiesberger Katrin, Christian Doppler Laboratory for Innovative Immunotherapy, Institute of Animal Breeding and Genetics, University of Veterinary Medicine, Vienna, Austria).

3.3.2 Media

- Dulbecco's Modified Eagle's Medium (DMEM) with High Glucose (4.5 g/l), supplemented with Stable Glutamine (PAA, # E15-883)

- Dulbecco's Modified Eagle's Medium / Nutrient Mixture F-12 [(DMEM/Ham's F-12 (1:1)] with Stable Glutamine (PAA, # E15-889)
- Roswell Park Memorial Institute 1640 medium with L-glutamine (RPMI 1640); (PAA, # E15-840)
- Fetal Bovine Serum (FBS) Standard Quality, EU-approved; heat-inactivated; (PAA, # A15-101)
- Normocin (50 mg/ml) (InvivoGen, # ant-nr-2)

3.3.3 Cell culture equipment

- Trypsin-EDTA (1:250, 1x; PAA, # L15-004)
- Dulbecco's Phosphate Buffered Saline (DPBS) with Calcium and Magnesium, sterile (PAA, # H15-001)
- 0.5 M EDTA, pH 8.0 (Life Technologies, # 15575020)
- DPBS/EDTA: DPBS + 0.2 mM EDTA
- Freezing medium: 70 % fresh medium (corresponding to cell line)
  20 % FBS
  10 % endotoxin-tested dimethyl sulfoxide (DMSO) (Sigma-Aldrich, #472301)
- Tissue culture flasks, dishes, multi-well-plates, serological pipettes, 15 ml and 50 ml tubes, tips (Sarstedt)
- 0.2 µm Syringe Filter (Nalgene, # 176-0020)
- 0.45 µm Syringe Filter (Nalgene, # 176-0045)
- Cryovials (Greiner bio-one, # 123261)
- Haemocytometer (Neubauer)
- Trypan Blue Solution (Sigma-Aldrich, # T8154)

3.4 Lentiviral vector preparation

- Plasmid-mix: 2.4 µg HIV-pLP1
  5.7 µg HIV-pLP2
  1.2 µg pHCMV-G
  10 µg transfer vector (pLB-U-mCherry or pLB-U-mKate2)

- Transfection buffer A: 0.1 M HEPES (pH 7.0; Invitrogen, # 15630-056)
  0.5 M $CaCl_2$ (Merck, # 1023911000)
  mixed in Milli-Q water, adjusted to pH 7.0, filtered and stored at 4 °C
- Transfection buffer B: 0.05 M HEPES (pH 7.0)
  0.28 M NaCl
  0.75 mM NaH_2PO_4 (Sigma-Aldrich, # S0751)
  0.75 mM Na_2HPO_4 (Sigma-Aldrich, # 255793);
  mixed in Milli-Q water, adjusted to pH 7.0, filtered and stored at 4 °C

3.5 Infection and selection of recipient cells

- Blasticidin S-HCl (Invitrogen, # R210-01)
- Olympus IX70 UV-microscope equipped with an Olympus XM10 monochrome camera

3.6 Flow Cytometry and Fluorescence Activated Cell Sorting

3.6.1 Flow Cytometry for stability of RFP-expression

- BD FACSCalibur equipped with CellQuest software (Becton Dickinson)
- FACS buffer: 20 % FBS in DPBS

3.6.2 Cell sorting

- BD FACSAria (488-nm (blue) and 633-nm (red) lasers, 70 µm nozzle); equipped with BD FACSDiva software; (Becton Dickinson)

3.6.3 Flow cytometry for CSPG4-expression

- BD FACSCalibur; equipped with CellQuest software; (Becton Dickinson)
- Primary mouse monoclonal antibody directed against NG2/CSPG4 (NG2 Antibody (7.1): sc-53508, Santa Cruz Biotechnologies, # sc-53508)
- Secondary goat anti-mouse IgG-PE antibody (Jackson Immunoresearch, # 115-116-146)
- FACS buffer: 20 % FBS in DPBS

3.7 r28M-mediated *in vitro* cell killing

- Monomeric r28M antibody *12CDL12* (c = 5500 ng/µl) → extracted and purified from the CD-laboratory for Innovative Immunotherapy, University of Veterinary Medicine, Vienna, Austria.
- Dimeric r28M antibody *11PAKT04* (c = 970 ng/µl) → extracted and purified from the CD-laboratory for Innovative Immunotherapy, University of Veterinary Medicine, Vienna, Austria.
- Cell Proliferation Reagent WST-1 (Roche, # 05015944001)
- ELISA reader equipped with the SOFTmax PRO software

3.8 Western blot

3.8.1 Preparation of cell lysates and protein concentration determination

- 1 M Tris-HCl: 121.1 g Tris base (Sigma, # T6066) in 1 l $_{dd}H_2O$
- 3 M NaCl: 175.32 g NaCl (Sigma, # S 3014) with $_{dd}H_2O$ up to 1 l
- Lysis buffer: 50 mM TRIS-HCl
  50 mM NaCl
  0.5 % (w/v) sodium-deoxycholate (Sigma, # D6750)
  1 % (v/v) NP-40 (Igepal CA-630, Sigma, # I3031)
  adjusted to pH 7.4
- Protease Inhibitor Cocktail (PIC, Sigma-Aldrich, # P2714)
- Qubit 2.0 Fluorometer (InvitroGen)
- Qubit Protein Assay Kit (InvitroGen, # Q33211)

3.8.2 SDS gel electrophoresis

- Gel recipes:

Ingredients	7 % separation gel [ml]	4 % stacking gel [ml]
30 % Acrylamide/Bis Solution (29:1, 37.5:1) (Bio-Rad, # 161-0156)	1.420	0.3400
1 M Tris-HCl, pH 8.8	2.400	0.3150
10 % SDS (Merck, # 8170342500)	0.064	0.0250
$_{dd}H_2O$	2.230	1.8300
TEMED (Bio-Rad, # 161-0801)	0.005	0.0035
30 % Ammoniumpersulfate (APS) (Bio-Rad, # 161-0700)	0.033	0.0150

- Sample application buffer: 100 mg SDS
  0.5 ml 0.5 M Tris-HCl (pH 6.8)
  0.3 ml glycerol (Sigma, # G 5516)
  0.2 % bromophenol blue (Sigma-Aldrich, # B8026)
  800 mM DTT (Sigma, # D9163)
  in 2 ml $_{dd}H_2O$
- Bio-Rad Mini-Protean TetraSystem electrophoresis chamber
- Marker Novex Sharp Pre-stained Protein Standard (InvitroGen, # LC5800)
- Electrophoresis buffer: 30.92 g Tris-base
  144.13 g glycine (Merck, # 357002-1KG)
  10 g SDS
  in 1 l $_{dd}H_2O$

3.8.3 Protein transfer and detection

- Bio-Rad Criterion Blotter
- Protran Nitrocellulose blotting membrane (0.2 µm; Whatman, # 10401396)
- Criterion Blotter Filter Paper (Bio-Rad, # 1704085)
- 5x Transfer buffer: 15 g Tris-base
  72 g glycine;
  diluted 1:5 with $_{dd}H_2O$, then add

20 % MeOH (Sigma-Aldrich, # 459828)

- Ponceau Red solution: 0.5 % Ponceau S (AppliChem, # A1405,0025)
  5 % acetic acid (Sigma-Aldrich, # P7754)
- Fixation buffer: 50 % MeOH, 5 % acetic acid
- Sensitizing buffer: 0.02 % $Na_2S_2O_3$ (Sigma-Aldrich, # S7026)
- Silver solution: 0.1 % $AgNo_3$ (Sigma-Aldrich, # 38310)
- Developer: 0.05 % formaldehyde (Sigma-Aldrich, # 47608) in
  3% Na_2CO_3 (Sigma-Aldrich, # S4132)
- Stopping solution: 5 % acetic acid
- 1 x TBS: 50 mM Tris-HCl (pH 8.0)
  150 mM NaCl
- 1 x TBS-T: 0.05 % Tween 20 (Sigma-Aldrich, # P9416) in 1 x TBS
- Blocking solution: 4 % milk powder
  1 % BSA (Sigma-Aldrich, # A9418)
  in 1 x TBS
- Primary antibody dilution: NG2 Antibody produced in rabbits (Cell Signaling, # 4235); 1:1000 in 5% w/v BSA and 1x TBS-T
- Secondary antibody dilution: anti-rabbit IgG (whole molecule) – Peroxidase antibody produced in goat (Sigma, # A0545); 1:2000 in TBS-T and 5 % w/v milk powder
- Beta-actin detection mix: primary anti-beta-actin antibody (1:20000, Abcam, # ab6276) and secondary goat anti-mouse IgG1 heavy chain (HRP) antibody (1:2000; Abcam, # ab98693) in TBST with 5 % w/v BSA
- Pierce ECL Western Blotting Substrate Kit (ThermoScientific, #32209)
- Densitometric analysis with ImageJ. Link: http://rsb.info.nih.gov/ij/

3.9 *In vivo* experiments

- 10 female mice of the NOD.Cg-Prkdc^{scid} Il2rg^{tm1Wjl}/SzJ (NSG) strain (obtained by Biomodels Austria, University of Veterinary Medicine, Vienna, Austria).

- Anaesthesia: 1.00 mg Ketamine (Sigma-Adrich, #1867-66-9)
  0.04 mg Xylazine (Sigma-Aldrich, #23076-35-9)
  per 10 g mouse
- Lab Standard Stereotaxic Instrument with Mouse and Neonatal Rat Adaptor (Stoelting, # 51615), coupled to Quintessential Stereotaxic Injector (Stoelting, # 53311)
- IVIS Spectrum Pre-clinical In Vivo Imaging System (IVIS 50; PerkinElmer, # IVISSPE)

4 METHODS

4.1 Transformation of bacteria and plasmid DNA isolation

Transformation competent *E.Coli* bacteria were transformed with the plasmids needed for virus vector construction (HIV-pLP1, HIV-pLP2, pHCMV-G, pLB-U-mCherry and pLB-U-mKate2) according to the New England Biolabs' protocol. Briefly, the cells were thawed on ice and 100 ng of plasmid was added. Heat shock was performed for 45 seconds at 42 °C. Transformants were selected on lysogeny broth (LB) agar containing 0.1 µg/ ml ampicillin.

Extraction and purification of the plasmid DNA was performed according to the QIAGEN Plasmid Maxi Kit Purification protocol. Briefly, the overnight culture was pelleted at 6,000 xg for 15 minutes at 4 °C and resuspended in 10 ml of lysis buffer P1. Total lysis of the bacteria was done with 10 ml of buffer P2. After 4-5 minutes 10 ml of neutralization buffer P3 was added and mixed by roughly inverting. After incubation for 20 minutes on ice, the sample was centrifuged at 20,000 rpm for 30 minutes at 4 °C and the supernatant was immediately transferred into an equilibrated QIAGEN-tip 500 column. The column was washed twice with 30 ml buffer QC and elution of the plasmid DNA was done with 15 ml of elution buffer QF. The plasmid DNA was precipitated with 10.5 ml room-tempered isopropanol and washed with 70 % ethanol at 15,000 xg for 15 minutes. The dried pellet was dissolved in 500 µl $_{dd}H_2O$ and stored in the fridge.

Plasmid DNA concentration was estimated with a NanoDrop 1000 spectrophotometer.

4.2 Restriction digestion and agarose gel electrophoresis

0.5 - 1 µg of the pDNA was taken for restriction enzyme digestion using the appropriate conditions given by the restriction enzyme's manufacturer. According to the different plasmid sizes, the percentage of the agarose in the gel and the voltage were chosen. Different DNA markers and 6x Orange loading dye solution were used to visualise the bands in order to analyse the fragment lengths. A Tris-acetate-EDTA (TAE) buffer was used as electrophoresis buffer. The gel was kept

in a 1 % ethidium bromide bath for 15 minutes before pictures were taken under UV-light.

4.3 Cell culture

Human embryonic kidney cells (HEK-293T) were grown in DMEM with high glucose (4.5 g/l) supplemented with stable glutamine and 10 % heat-inactivated fetal calf serum (FCS). The human skin melanoma cell line SK-MEL-28 was kept in DMEM/Ham's F-12 with L-glutamine and 10 % FCS. A-375 cells were cultured in DMEM with 10 % FCS. The human melanoma cell line IPC-298 was kept in RPMI 1640 medium with L-glutamine and 10 % FCS. If indicated, 50 mg normocin per ml medium was added to all media. All cell lines were cultured at 37 °C in a humidified atmosphere containing 5 % CO_2. Cell cultures were regularly checked for visible contaminations under an optical microscope.

4.3.1 Passaging of cells

If not indicated otherwise, splitting of the cells was done when their confluence was reached. Therefore, the medium was aspirated and the cells were washed with Dulbecco's Phosphate Buffered Saline (DPBS). Cells were detached by adding either 1x Trypsin-EDTA or DPBS-EDTA followed by incubation at 37 °C for 5-10 minutes. For neutralisation fresh medium was added and the respective volume of cell suspension was resuspended in corresponding full medium.

4.3.2 Freezing of cells

For the preparation of frozen cell stocks, cells were detached and resuspended in a corresponding fresh medium as described above. Cells were pelleted by centrifugation at 1,500 rpm for 5 minutes at room temperature. The cell pellet was resuspended in corresponding freezing medium and transferred into cryovials. To obtain slow freezing, the cells were put into a Styrofoam box at -80 °C for 24 hours, before they were taken out of the box and placed deep inside the -80 °C freezer.

4.3.3 Cell counting

Counting of the cells was performed in a haemocytometer according to the manufacturer's instructions. For killing assays a viable cell count with the use of trypan blue was done. Therefore 10 µl of trypan blue was mixed with 10 µl cell solution and incubated for 5 minutes at 37 °C before cells were counted.

4.4 Lentiviral vector preparation

The HEK-293T cells were seeded into a 10 cm dish at a density of 5 x 10^6 cells per 10 ml medium. After 24 hours the plasmid-mix containing the lentiviral components (HIV-packaging plasmid pLP1, rev-containing plasmid pLP2, VSV-G envelope containing plasmid pHCMV-G and transfer vectors) were filled up to a total volume of 240 µl with $_{dd}$H2O. Cold transfection buffer A was added in the same amount and the sample was vortexed and incubated for 10 minutes at room-temperature. Afterwards cold transfection buffer B was added drop wise. The sample was again vortexed, incubated for 15 minutes at room-temperature, mixed by inversion and added drop wise onto the cells in the 10 cm dish. 24 hours later the medium was replaced by 10 ml of fresh medium. 48 hours after the medium change the virus-containing supernatant was harvested, filtered through a 0.45 µm filter and frozen at -80 °C.

4.5 Infection and selection of recipient cells

Recipient tumour cells were seeded into 6 cm dishes at a density of 4 x 10^5 per 5 ml medium. On the next day 3 ml of the medium was aspirated and infection was done by adding 500 µl of the virus-containing supernatant to the cells. For each type of melanoma cell, a 6 cm dish remained uninfected to serve as a negative control. When the cells had reached confluence they were transferred into T75 culture flasks in which selection of the transduced cells using blasticidin was started 24 hours later.

Prior to the selection of infected cells, the minimal killing dose of blasticidin was estimated. For this purpose the A-375, SK-MEL-28 and IPC-298 cells were seeded into 6-well plates at a density of 5 x 10^4 cells in a total volume of 3 ml medium per well. On the next day different concentrations of blasticidin (3, 5, 7, 10

or 12 µg/ml) were added to the wells. The medium was replaced with fresh blasticidin-containing selection medium after 3 days of incubation, and then left for further 3 days. Based on light microscopy the minimal killing dose for each cell line was estimated according to the well in which cells had been killed completely during selection procedure.

To obtain population of stably infected melanoma cells, the estimated minimal killing dose of blasticidin was applied onto the cells infected with the *mKate2*- or *mCherry*-containing lentiviral vectors. 3-4 weeks after infection, blasticidin was withdrawn from the medium and the cells were cultivated in normal growth medium containing normocin.

4.6 Flow cytometry and Fluorescence-activated cell sorting

To estimate the amount of infected cells as well as to detect CSPG4-expression on the melanoma cells, flow cytometry was used. Infected melanoma cells, if needed, were sorted in a Fluorescence Activated Cell Sorter (FACS).

4.6.1 Flow cytometry for stability of RFP-expression

To evaluate the number of cells expressing the fluorescence protein, cells were detached, resuspended in fresh medium and centrifuged at 2,000 rpm for 2 minutes at room temperature. The cells were washed twice by resuspending the pellet in DPBS followed by repeated centrifugation at 2,000 rpm for 2 minutes at room-temperature. The pellet was resuspended in 800 µl FACS-buffer and the percentage of fluorescent protein expressing cells as well as the mean fluorescence intensity (MFI) was measured in the fluorescence activated cell sorter.

4.6.2 Cell sorting

If the desired number of RFP-expressing cells could not be obtained after infection, cell populations positive for RFP-expression were enriched by means of FACS sorting. Therefore, cells were detached, washed once in DPBS, centrifuged at 2,000 rpm for 4 minutes at room temperature and resuspended in FACS buffer. Cells were then sorted according to their RFP-expression. MFI threshold level was

chosen in respect to the fluorescent proteins expressed by the different cell lines. 1 x 10^6 RFP-expressing cells were sorted out and seeded into a T75 flask in corresponding fresh medium containing normocin.

4.6.3 Flow cytometry for CSPG4-expression

To analyse the presence of the CSPG4 antigen in parental and transduced tumour cells, they were washed with DPBS and incubated at 37 °C with DPBS/EDTA. Final detaching was done by pipetting up and down directly onto the bottom of the culture flasks. The cells were transferred into tubes containing 1 ml fresh medium per 10 ml cell suspension and centrifuged at 1,000 rpm for 5 minutes at room temperature. The pellet was resuspended in DPBS before the cells were counted and divided into tubes containing 1 x 10^6 cells per tube. After repeated centrifugation, the pellet was washed twice with 500 µl FACS-buffer. The cells were incubated with 1 µg of the primary mouse monoclonal antibody directed against CSPG4/NG2 per 1 x 10^6 cells for 45 minutes at 4 °C.

Afterwards the samples were washed twice in FACS-buffer before 5 µg of the secondary goat anti-mouse IgG antibody conjugated to phycoerithrin was added per ml sample and incubated for 45 minutes at 4 °C in the dark. After washing the cells were resuspended in 800 µl FACS-buffer and analysed in the FACSCalibur. Corresponding controls lacking primary or secondary antibodies were analysed as well.

4.7 Growth kinetics analysis

To investigate possible alterations in growth due to infection with lentiviral vectors, the parental as well as the transduced melanoma cells were detached, counted and seeded into 6-well plates at a density of 2 x 10^5 cells per 4 ml corresponding medium. Each day the cells of one well were counted and the total cell number was determined until confluence was reached. Using the software MS Excel the cultivation time (in hours) was plotted against the logarithmic values of the total cell number counted at each day. To determine the logarithmic phase of the curve, an exponential regression analysis was performed. The growth rate was obtained from the equation: $amount = x * e^{y*time}$, x representing the cell

concentration at the time point of seeding and y representing the growth rate (number of doublings that occur per unit of time). The doubling time (t) was then calculated as follows: $t = \ln(2) / y$.

4.8 r28M-mediated *in vitro* cell killing

To determine the effect of the r28M antibody on tumour cell viability, parental and transduced melanoma cells were passaged 24 hours before they were used for killing assay. On the next day cells were harvested by washing them twice with DPBS, detaching by DBPS/EDTA and neutralizing in growth medium. After spinning for 4 minutes at 2,000 rpm cells were resuspended in fresh medium, counted and seeded in a 96-well-plate at a density of 1 x 10^4 cells per 50 µl medium per well. Peripheral Blood Mononuclear Cells (PBMCs) were also counted and added to the tumour cells at a density of 1 x 10^5 cells per 50 µl medium per well to obtain an effector-target-ratio of 10:1. Next, three different concentrations of the r28M antibody (50, 500 and 5000 ng / well of the monomeric r28M and 1000, 100 and 10 ng / well for the dimeric r28M) were tested.

Wells containing solely either PBMCs, medium or tumour cells, as well as wells containing tumour cells together with PBMCs and wells containing tumour cells together with the antibody were seeded to serve as controls. After bringing the volume of each well to the same volume of 150 µl by adding the respective amount of medium, the 96-well plate was wrapped in plastic foil and incubated at 37 °C and 5 % CO_2. 72 hours later the medium was aspirated, and the wells were washed twice with DPBS. Water soluble tetrazolium (WST-1), diluted 1:10 with complete medium, was added to each well and incubated for 1.5 hours in the dark. Optical density (OD) was determined using an ELISA reader. Since these experiments were performed in quadruplets, the percentage of killed cells was calculated according to Grosse-Hovest et al. $(1 - A_x / A_{max}) * 100$, where A_{max} is the optical density generated by tumour cells in the absence of antibodies. A_x and A_{max} are values diminished by the background that is generated by medium containing the WST dye only.[25]

4.9 Western blot

To detect possible changes in the expression of CSPG4 on infected melanoma cells, a Western blot for this protein was performed.

4.9.1 Preparation of cell lysates and protein concentration determination

Cells were washed with DPBS, detached by DPBS/EDTA, neutralized with fresh medium and pelleted at 2,000 rpm for 4 minutes at room-temperature. Lysis was performed by resuspending the pellet in 100 µl lysis buffer per 2 x 10^6 cells followed by incubation on ice for 45 minutes. Cleared cell lysates were obtained by spinning at 15,000 rpm for 20 minutes at 4 °C and frozen at -20 °C. The concentration of total amount of proteins in the lysates was determined using the Qubit 2.0 Fluorometer.

4.9.2 SDS gel electrophoresis

For separating the proteins according to their sizes, a 7 % separation gel and a 4 % stacking gel were casted into an electrophoresis chamber. 20 µg of the cell lysates were mixed with 5 x sample application buffer, boiled for 5 minutes at 95 °C and loaded onto the gel. Gel electrophoresis was performed at 160 Volt.

4.9.3 Protein transfer and detection

For the semi-dry transfer of proteins onto a nitrocellulose transfer membrane, the blotter was assembled according to the manufacturer's instructions. Transfer was performed at 60 Volt for 2 hours. Afterwards the membrane was stained with Ponceau Red solution for 3 – 5 minutes, washed with $_{dd}H_2O$ and scanned.

In addition, silver staining of the gel was performed. Therefore, the gel was incubated in fixation-buffer, first for 1 hour and then overnight in a fresh batch of buffer. On the next day the gel was washed and sensitizing was done for 1 minute in sensitizing buffer, before the gel was washed twice with $_{dd}H_2O$ for 1 minute. Silver impregnation was obtained by incubating the gel in cold silver nitrate solution for 20 minutes in the dark. Prior to putting the gel into developer solution until the adequate degree of staining had been achieved, it was rinsed twice with

$_{dd}H_2O$, and then washed in $_{dd}H_2O$ for 1 minute. The precipitate that developed after a few seconds in the developer solution was re-dissolved by shaking the developer/gel-containing box. Then the gel was transferred into stopping solution for 30 minutes, before washed twice in $_{dd}H_2O$ for 30 minutes.

The destained membrane was incubated in blocking solution at 4 °C on a shaker overnight. On the next day the blocked membrane was incubated in primary antibody dilution (1: 1000) at 4 °C on a rotation shaker overnight.

On the next day the membrane was rinsed twice with wash buffer before washed 5 x 5 minutes on a shaker and incubated in secondary antibody dilution (1: 2000) for 1 hour at room temperature. The membrane was rinsed twice with wash buffer before washed 5 x 5 minutes on a shaker. At last the membrane was washed twice in TBS for 5 minutes.

To verify loading of equal amounts of protein, the membrane was incubated in beta-actin detection mix (primary anti-beta-actin antibody 1: 20000 mixed with secondary HRP-conjugated antibody 1: 2000) for 15 minutes at room temperature before the same washing procedure as after incubation with the secondary antibody dilution was done. For detection of CSPG4 luminol/enhancer solution and peroxidase buffer were mixed 1:1 and added onto the membrane. After 1 minute the excess of the solution was removed and the membrane was placed in a plastic sheet protector before the X-ray film was developed.

4.10 Test for tumourigenicity in mice

All animal experiments were approved by the institutional ethics committee and the Austrian government authorities; BMWF-68.205/0174-II/3b/2012. Animal work was carried out by Hlavaty Juraj, CD-laboratory for Innovative Immunotherapy, University of Veterinary Medicine, Vienna, Austria.

Briefly, tumourigenicity of human cells was analysed in immune-deficient NOD.Cg-Prkdcscid Il2rgtm1Wjl/SzJ (NSG) mice. Growing brain tumours were obtained after direct injection of 1 x 10^6 melanoma cells into the mouse brain at 1 mm anterior and 1.5 mm lateral to bregma and 3.5 mm deep.

In vivo visualisation of tumours was performed with the IVIS-50 system in anaesthetised animals.

5 RESULTS

5.1 Plasmid preparation and restriction digestion

To obtain the required amounts of the lentiviral components (HIV-pLP1, HIV-pLP2, pHCMV-G, pLB-U-mCherry and pLB-U-mKate2) *E.coli* bacteria were transformed with those plasmids via heat-shock method. Transformants were selected on ampicillin-containing agar. The isolated pDNA products were verified via restriction digestion.

As a representative example the band pattern for HIV-pLP1 after restriction digestion and gel electrophoresis is shown in Figure 5. The expected fragment length of 4335 bp, 4153 bp and 401 bp for digestion with EcoRI; 7465 bp and 1424 bp for digestion with PstI; and 8776 bp for digestion with SacI could be obtained.

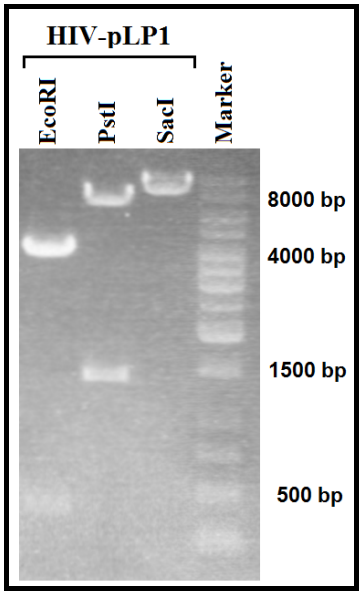

Figure 5. Gel picture of HIV-pLP1 plasmid band pattern after isolation and restriction digestion. The expected bands were produced by different restriction enzymes.

5.2 Lentiviral vector preparation

HEK-293T cells were transformed with the lentiviral vector plasmids as explained in the Methods section. The lentiviral vector-containing supernatant was used immediately or stored at -80 °C.

5.3 Infection of recipient cell lines and stability of fluorescence protein expression

The human melanoma cell lines A-375, SK-MEL-28 and IPC-298 were infected with lentiviral vectors containing the fluorescent genes, followed by their selection with blasticidin. In order to estimate minimal killing concentration of blasticidin, cells were incubated in medium containing different amounts of blasticidin. Based on light-microscopy the minimal killing dose turned out to be 5 µg per ml medium for the SK-MEL-28 and IPC-298 cells, whereas the A-375 cells were killed with a blasticidin-concentration of 3 µg per ml medium.

To evaluate the number of melanoma cells expressing the mCherry or mKate2 protein as well as the stability of the expression, the percentages of parental and infected melanoma cells positive for RFP-expression were estimated regularly by flow cytometry.

In the case of the A-375 cells, the number of RFP-expressing cells, as well as the stability of the expression after blasticidin-selection was sufficient for further testing. About 95 % of the blasticidin-selected A-375 cells transduced with *mCherry* and 75 – 85 % of the blasticidin-selected A-375 cells transduced with *mKate2* revealed stable expression, which was measured for more than 170 days (Figure 6.A).

In contrast, the transduced SK-MEL-28 and IPC-298 cell lines revealed neither high numbers of RFP-expressing cells, nor stable expression rates after blasticidin-selection. In case of the *mKate2*-transduced SK-MEL-28 and IPC-298 cells low numbers of RFP-expressing cells (about 60 % for SK-MEL-28 cells and 25-35 % for IPC-298 cells, data not shown) could be revealed. The same cell lines transduced with *mCherry* showed high numbers of positive cells after blasticidin-selection (about 85 % for SK-MEL-28 cells and 80 % for IPC-298 cells, data not shown). However, starting on day 40, the percentages of *mCherry*- expressing SK-MEL-28 cells decreased significantly (between 7 and 10 % at each measurement, up to a total decrease of 55 % in 50 days; data not shown). Likewise, starting at day 80, a steady decrease in cells positive for *mCherry*-expression was observed in the IPC-298 cells (2-8 % at each measurement, a total of 20 % decrease in 30 days; data not shown).

Due to the low numbers of RFP-expressing cells and/or unstable expression of the fluorescence proteins after blasticidin-selection, the SK-MEL-28 and IPC-298 cells transduced with *mCherry* or *mKate2* additionally were sorted by FACS. After cell sorting the number of RFP-expressing cells as well as their MFIs increased (data not shown). Moreover the expression remained stable over several passages after sorting. About 90 % of the *mCherry*- and *mKate2*-transduced SK-MEL-28 cells revealed stable RFP-expression for 65 and 100 days respectively (Figure 6.B). Similar, for IPC-298 cells transduced with *mCherry* or *mKate2* sufficient numbers of RFP-expressing cells were obtained after cell sorting. At least 90 % of the *mCherry*-transduced IPC-298 cells showed a stable transduction rate for 80 days. In the case of the FACS sorted IPC-298-i-LB-U-mKate2 cells about 90 % displayed RFP-expression until day 68 (Figure 6.C). When this cell line was measured regularly until day 100, a slow decrease could be observed (Figure 6.C). Summarized data of RFP-expression of A-375 as well as of sorted SK-MEL-28 and IPC-298 cells transduced with the genes for mCherry or mKate2 are shown in Table 1.

Furthermore, FACS analysis revealed that the mean fluorescence intensities of *mCherry*-transduced cell lines were higher than those for the same cell lines transduced with *mKate2* (data not shown).

A

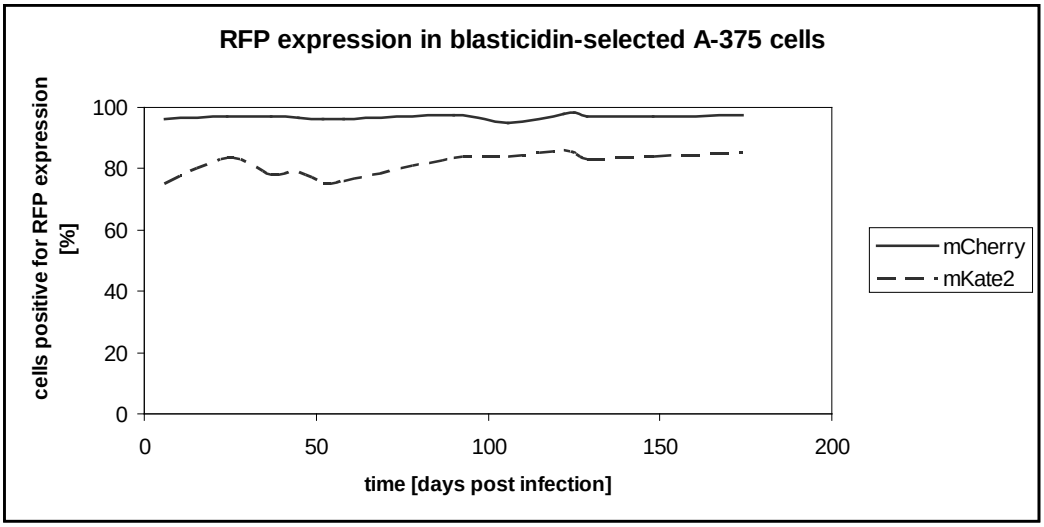

B

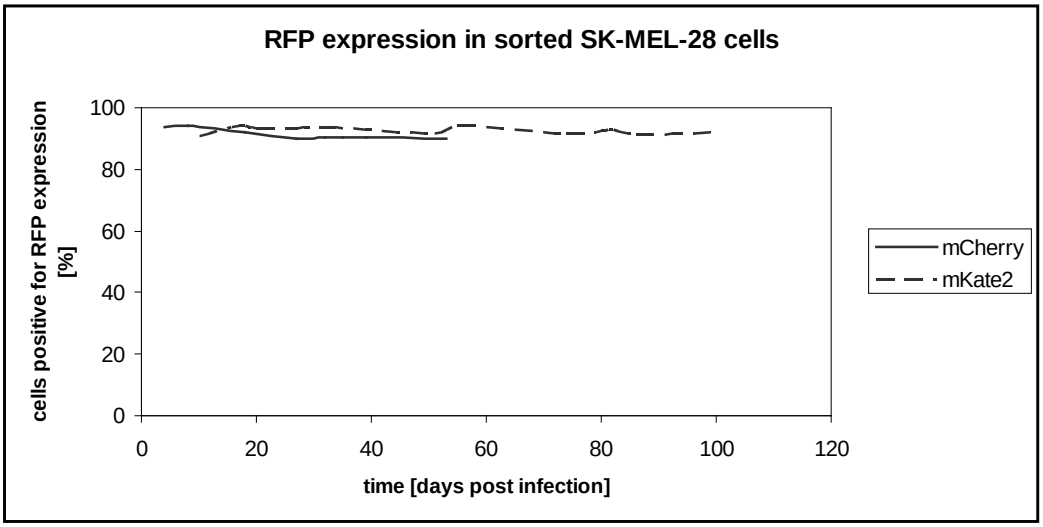

C

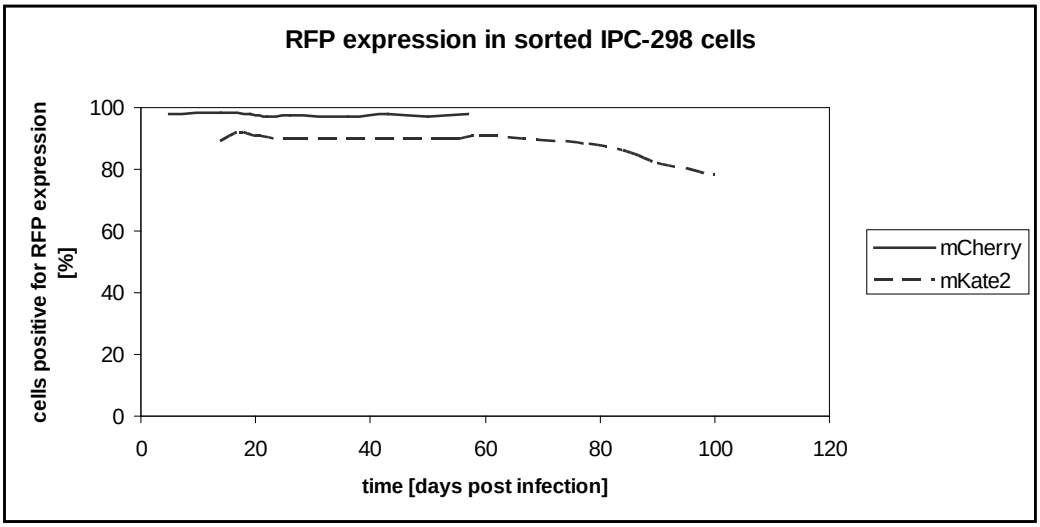

Figure 6. Number of fluorescent cells and stability of RFP-expression. A. After blasticidin-selection high percentages of fluorescence positive A-375 cells could be revealed. The expression of the RFPs was stable. **B.-C.** After FACS-sorting of cells, high numbers of *mCherry*- and *mKate2*-transduced SK-MEL-28 and IPC-298 cell lines displayed stable expression of the respective fluorescence proteins.

Cell line	Average value of RFP-expressing cells [%]
A-375-i-LB-U-mCherry	95
A-375-i-LB-U-mKate2	80
SK-MEL-28-i-LB-U-mCherry sorted	90
SK-MEL-28-i-LB-U-mKate2 sorted	90
IPC-298-i-LB-U-mCherry sorted	95
IPC-298-i-LB-U-mKate2 sorted	90

Table 1. Percentages of melanoma cells expressing mCherry or mKate2. The results obtained by flow cytometry for A-375 mCherry- or mKate2-positive cells after blasticidin-selection and for respective SK-MEL-28 and IPC-298 cells after FACS sorting are shown. Each cell line displayed stable RFP-expression if measured for at least 7 weeks.

To further support data obtained by FACS analysis, cells were visualised by fluorescence microscopy and representative pictures of each cell population were taken (Figure 7).

Generally, trends for the number of fluorescent cells in the different cell populations as revealed by FACS analysis as well as the differences in the brightness of *mCherry*- and *mKate2*-transduced cells were also noticed upon visualisation under a UV-microscope.

In the case of blasticidin-selected A-375-i-LB-U-mCherry cells, almost all expressed the red fluorescence protein, as documented in Figure 7.A.3. Given the same exposure time, the fluorescence intensity of the blasticidin-selected A-375-i-LB-U-mKate2 cells appeared weaker than the fluorescence intensity given by the *mCherry*-transduced A-375 cells (Figure 7.B.2). Moreover, the transduction rate for the *mKate2*-transduced A-375 cells was lower than for the *mCherry*-transduced A-375 cells (Figure 7.B.3).

Sorted SK-MEL-28 cells transduced with *mCherry* also showed higher fluorescence intensities, when compared to the sorted SK-MEL-28-i-LB-U-mKate2 cells (Figure 7.C.2 and Figure 7.D.2), whereas the number of RFP-expressing cells was similar in both populations (Figure 7.C.3 and Figure 7.D.3).

In case of the sorted IPC-298-i-LB-U-mCherry cells the fluorescence intensity as well as the transduction rate were higher than for the FACS sorted IPC-298-i-LB-U-mKate2 cells (Figure 7.E.2; E.3 and Figure 7.F.2; F.3).

A. A-375-i-LB-U-mCherry

A.1

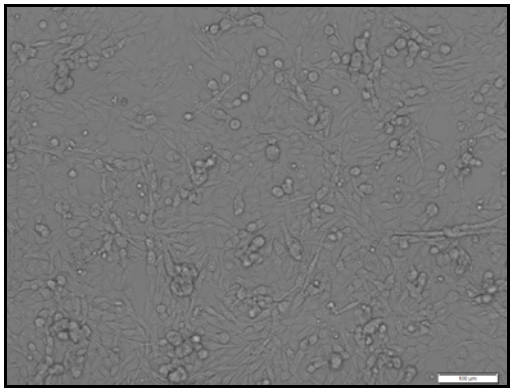

A.2

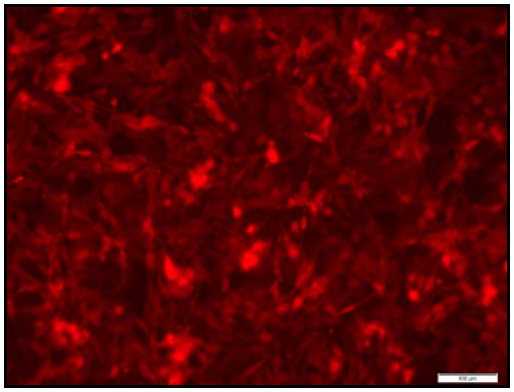

A.3

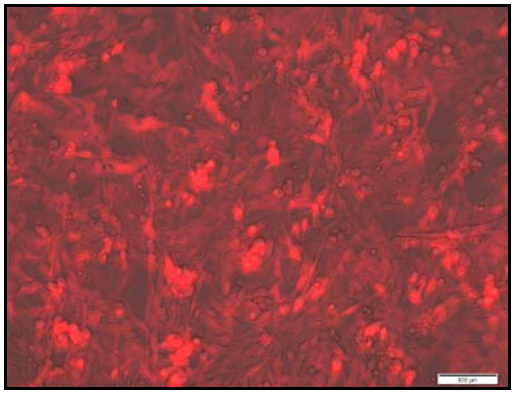

B. A-375-i-LB-U-mKate2

B.1

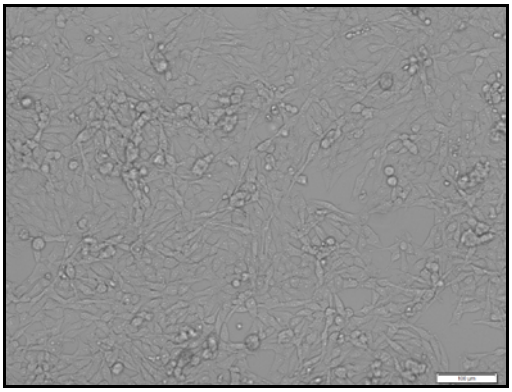

B.2

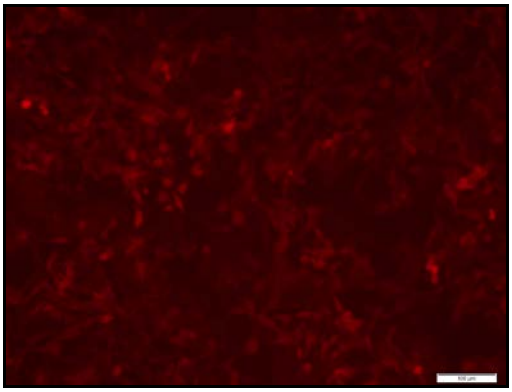

B.3

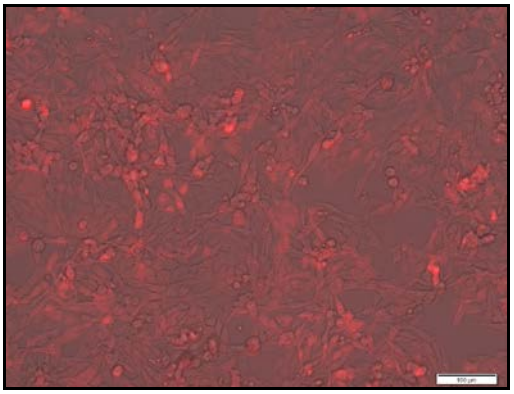

C. SK-MEL-28-i-LB-U-mCherry

C.1

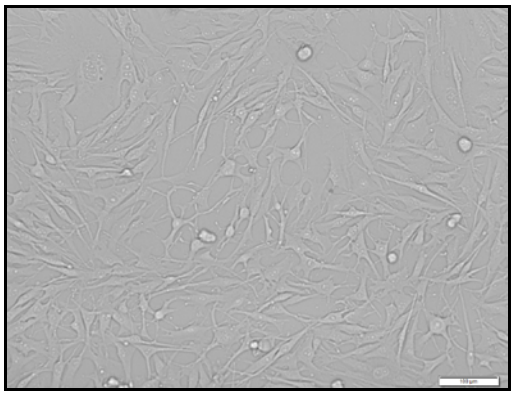

C.2

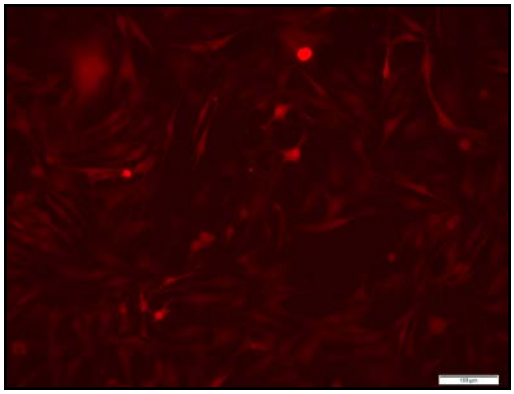

C.3

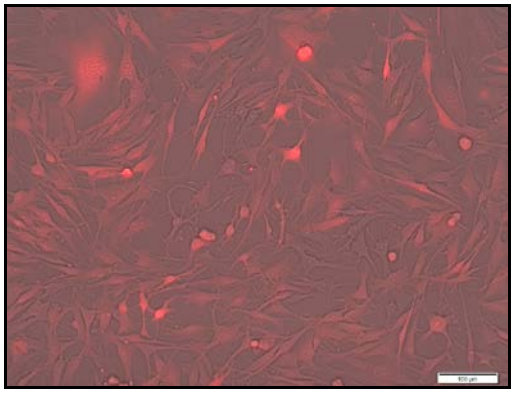

D. SK-MEL-28-i-LB-U-mKate2

D.1

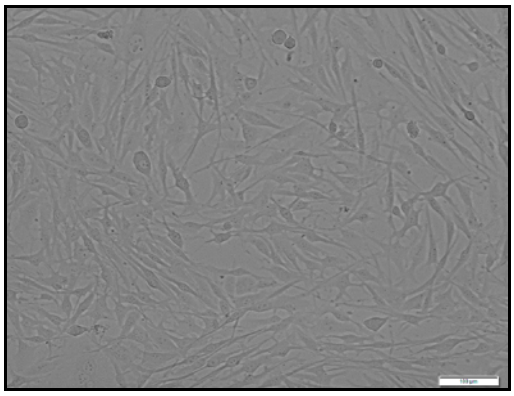

D.2

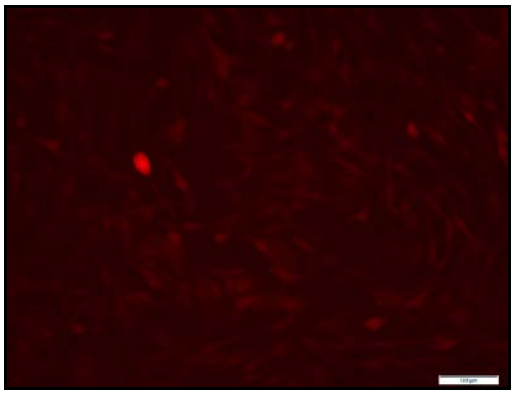

D.3

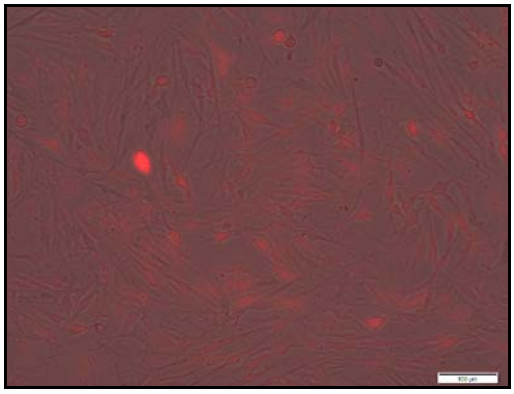

E. IPC-298-i-LB-U-mCherry

E.1

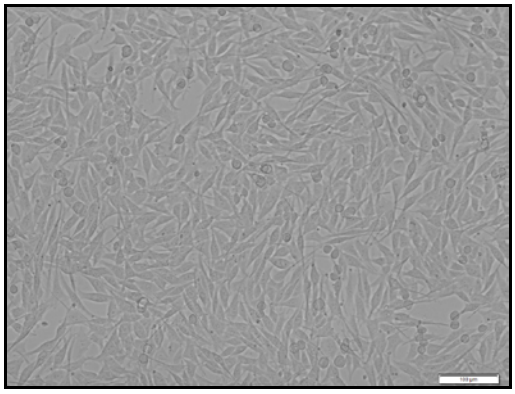

E.2

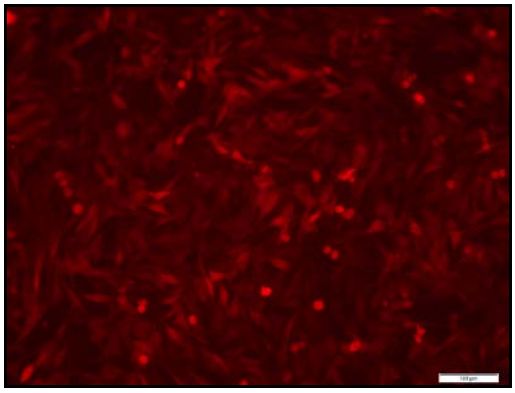

E.3

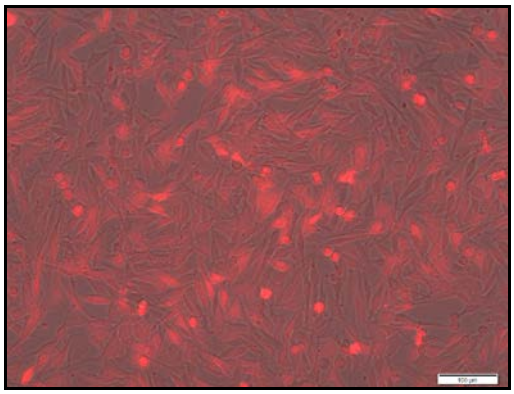

F. IPC-298-i-LB-U-mKate2

F.1

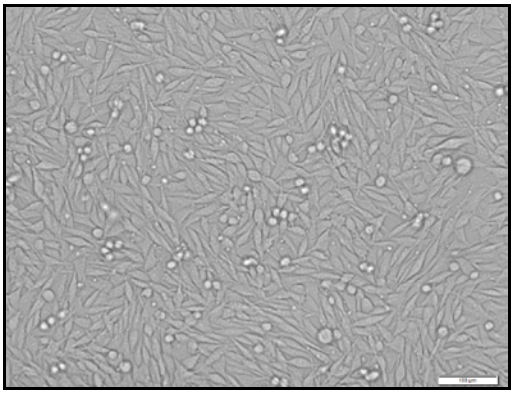

F.2

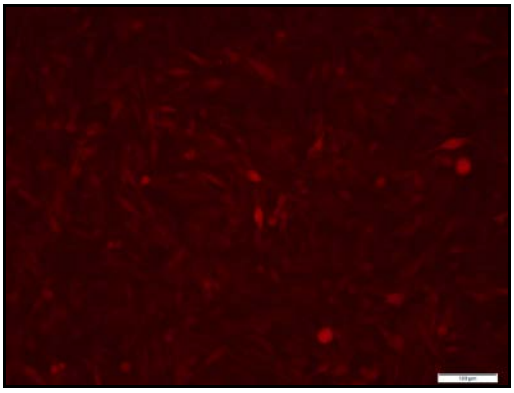

F.3

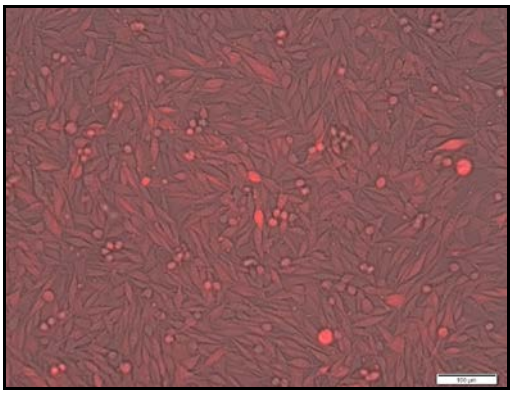

Figure 7. Lentivirally transduced melanoma cells expressing mCherry or mKate2 as observed by fluorescence microscopy. A.1, B.1, C.1, D.1, E.1 and F.1. Total cells under brightfield exposure. **A.2, C.2, E.2.** mCherry–expressing melanoma cells at an exposure time of 781 ms. **B.2, D.2, F.2.** mKate2–expressing melanoma cells at the same exposure time. **A.3, B.3, C.3, D.3, E.3, F.3.** Combined pictures of fluorescent cells with total cells, in which almost every cell appeared to be transduced with the gene for the respective fluorescent protein. Moreover, the *mCherry*-transduced melanoma cells were brighter than the *mKate2*-transduced ones **(A.2, C.2, E.2, and B.2, D.2, F.2)**.

Summarising, we can say that infections of the melanoma cell lines A-375, SK-MEL-28 and IPC-298 with *mCherry*-containing viruses resulted in higher fluorescence intensities than observed after infection with *mKate2*-containing viruses. For each RFP-expressing cell line a stable transduction rate was measured for several weeks. In case of the A-375 cells these data were acquired after blasticidin-selection, whereas the SK-MEL-28 and IPC-298 cells additionally were sorted. For further experiments the blasticidin-selected A-375 cells as well as the FACS-sorted SK-MEL-28 and IPC-298 cells, each transduced with the genes for mCherry or mKate2, were used.

5.4 Growth kinetics analysis

In order to exclude an effect of virus transduction or transgene expression on growth behaviour of the transduced cells, the growth kinetics of infected and parental cell lines were estimated. Briefly, known numbers of parental as well as *mCherry*- and *mKate2*-transduced melanoma cell lines A-375, SK-MEL-28 and IPC-298 were seeded and counted each day until they reached confluence. The growth rates and the doubling times were calculated as explained in the Methods section. The growth curves and doubling times for parental and transduced melanoma cells are summarised in Figure 8. The parental A-375 and SK-MEL-28 cells revealed doubling times of about 20 hours, whereas the mCherry- and mKate2-positive cells grew only slightly faster (Figure 8.A and Figure 8.B). The parental IPC-298 cells revealed doubling times of about 25 hours, whereas the growth kinetics of *mCherry*- and *mKate2*-transduced IPC-298 cells was slightly decreased (Figure 8.C). The differences in the doubling times between parental and transduced cell lines were below 7 % in all cases, whereupon they were considered as statistically insignificant.

A

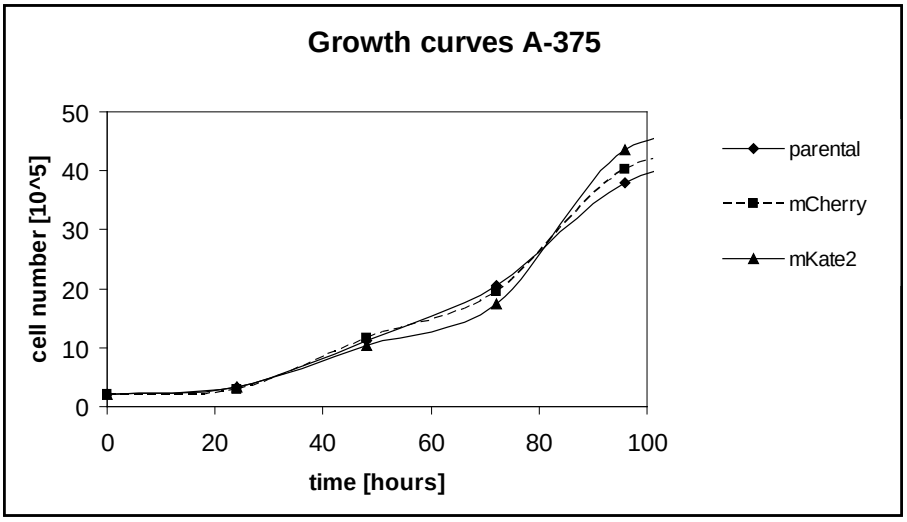

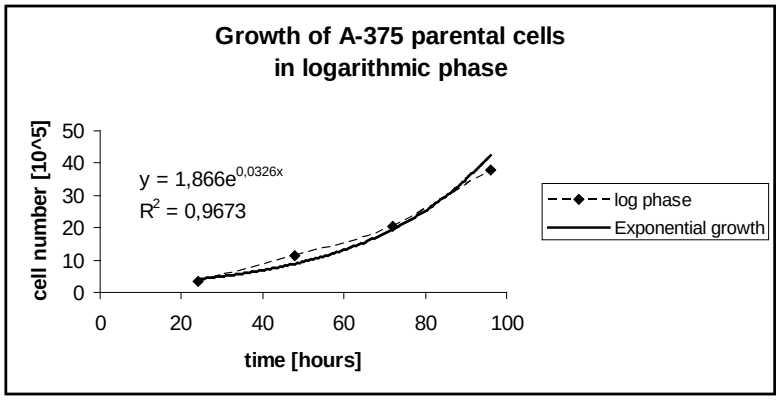

Cell line	Linear equation	R^2	Growth rate	Doubling time [h]	Difference in doubling time to parental cell line [%]
A-375 parental	$y = 1.866e^{0,0326x}$	0.97	0.0326	21.3	
A-375-i-LB-U-mCherry	$y = 1.5729e^{0,0349x}$	0.96	0.0349	19.9	6.6
A-375-i-LB-U-mKate2	$y = 1.6335e^{0,0342x}$	0.98	0.0342	20.3	4.7

B

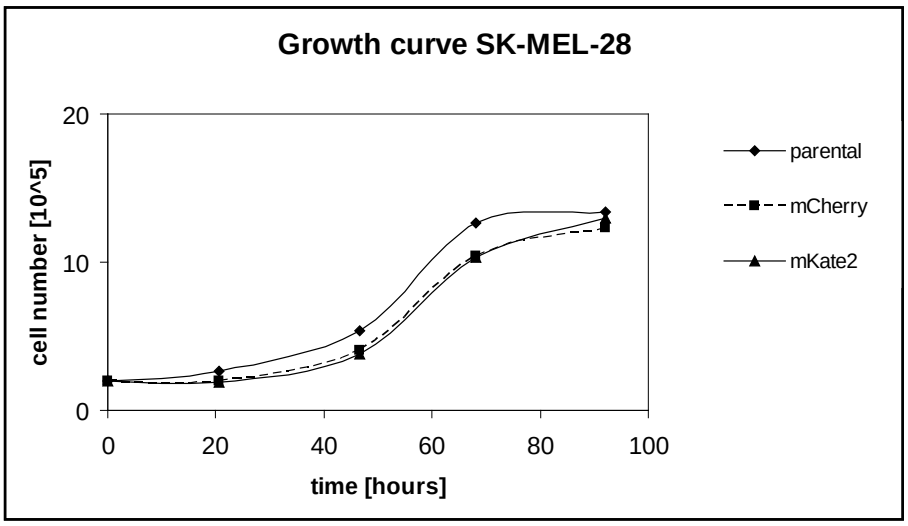

Cell line	Linear equation	R^2	Growth Rate	Doubling time [h]	Difference in doubling time to parental cell line [%]
SK-MEL-28 parental	$y = 1.271e^{0.0331x}$	0.99	0.0331	20.94	
SK-MEL-28-i-LB-U-mCherry sorted	$y = 0.9282e^{0.0345x}$	0.98	0.0345	20.09	4.06
SK-MEL-28-i-LB-U-mKate2 sorted	$y = 0.8803e^{0.0349x}$	0.97	0.0349	19.86	5.16

C

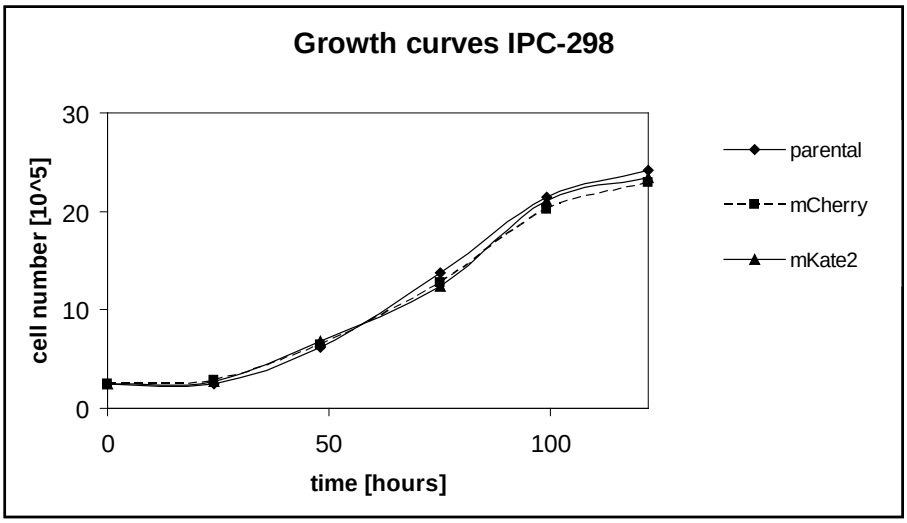

Cell line	Linear equation	R^2	Growth rate	Doubling time [h]	Difference in doubling time to parental cell line [%]
IPC-298 parental	$y = 1.4029e^{0.0287x}$	0.98	0.0287	24.76	
IPC-298-i-LB-U-mCherry sorted	$y = 1.6534e^{0.0262x}$	0.98	0.0262	26.46	6.87
IPC-298-i-LB-U-mKate2 sorted	$y = 1.6048e^{0.0268x}$	0.98	0.0268	25.86	4.48

Figure 8. Growth curves and doubling times of parental and transduced A-375, SK-MEL-28 and IPC-298 cells. Representative graphs and calculations are shown. Additionally, in **A.** the exponential growth phase of A-375 parental cells is shown exemplary. Each evaluated growth characteristic was similar between parental and transduced cells.

Thus, it can be concluded that each transduced cell line showed similar growth rate and similar doubling time to its parental cell line. We demonstrated that lentiviral infection and RFP-expression did not alter the growth kinetics of the melanoma cells.

5.5 Expression of CSPG4

In order to analyse the expression of the target antigen for the bispecific single-chain antibody r28M, flow cytometry as well as semi-quantitative Western blot was performed.

5.5.1 Analysis of CSPG4-expression by Flow Cytometry

To confirm the presence of the target antigen for the bispecific single-chain antibody r28M, named CSPG4, parental as well as transduced A-375, SK-MEL-28 and IPC-298 cells were labelled with a primary mouse monoclonal antibody directed against CSPG4 in combination with a secondary anti-mouse IgG antibody conjugated to phycoerithrin. The number of cells expressing CSPG4 was estimated by flow cytometry.

Almost 100 % of cells of all three cell lines were tested as CSPG4-positive. In addition, lentiviral transduction and RFP-expression did not alter the CSPG4-levels in infected cells.

5.5.2 Western blotting to detect level of CSPG4-expression

To further analyse the amount of CSPG4-expression, a semi-quantitative Western blot for this antigen was performed. Briefly, cell pellets were lysed with an NP-40 containing lysis buffer and loaded in equal amounts onto an SDS gel.

Semi-dry protein transfer followed by CSPG4 detection with the use of a primary anti-NG2 antibody and a secondary anti-rabbit HRP-conjugated antibody was performed. Beta-actin served as loading control. Since CSPG4 is a protein with a high molecular weight of about 255 kDa, the sufficient protein transfer from the gel onto the membrane is of high importance. To ensure this, membranes were stained with Ponceau red after transfer (Figure 9).

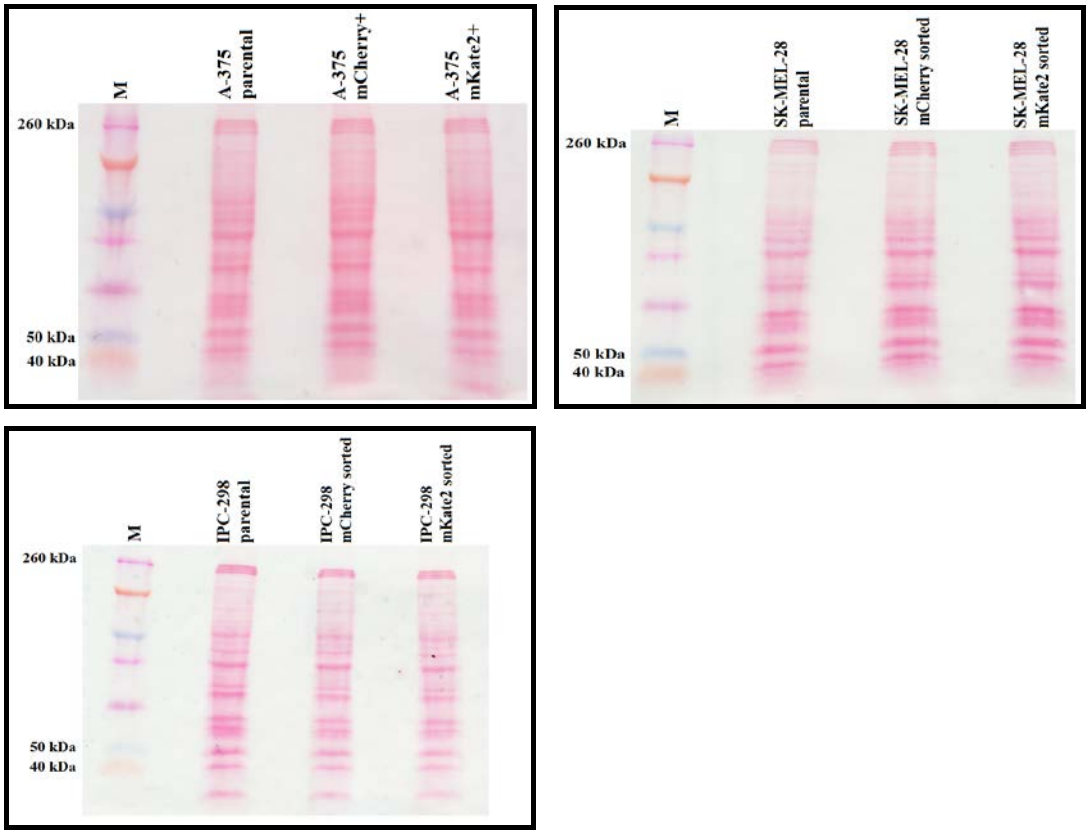

Figure 9. Ponceau staining. Transfer worked for low- as well as for high-molecular proteins, including CSPG4 with a molecular weight of about 255 kDa.

The detection of CSPG4 levels in parental and transduced A-375, SK-MEL-28 and IPC-298 cells is shown in Figure 10. Western blot data for CSPG4 in the A-375 cells revealed the brightest bands, which were detectable after exposure of the film for 30 seconds (Figure 10.A). In contrast, exposure time of 7 minutes was required to obtain distinct bands for the SK-MEL-28 cells (Figure 10.B) as well as for the IPC-298 cells, whereupon the latter revealed the weakest ones (Figure 10.C).

The amount of CSPG4-expression differed only marginally between the transduced cell lines and the respective parental cells. The A-375-i-LB-U-mCherry cells expressed 2.23 % and the A-375-i-LB-U-mKate2 cells 8.00 % more CSPG4 compared to parental cells (Figure 10.A). For the SK-MEL-28 cells the difference between parental to both transduced cell lines was about 3.5 % (Figure 10.B), whereas CSPG4-expression of both transduced IPC-298 cell lines revealed to be about 5 % lower as compared to the parental cells (Figure 10.C).

In summary, after Western blotting the amount of CSPG4-expression of *mCherry*- and *mKate2*-transduced A-375, SK-MEL-28 and IPC-298 melanoma cell lines revealed similar values as for expression of parental cells. Therefore, lentiviral transduction and expression of the RFPs did not change the expression level of the CSPG4 antigen in investigated cell lines. Moreover, transduced and parental A-375 cell lines showed highest expression, followed by SK-MEL-28 cells, whereas the IPC-298 cell lines displayed the lowest expression of all cell lines tested.

A

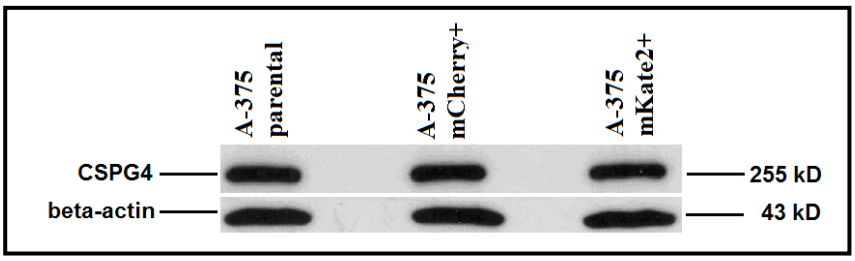

β-actin loading control	
Cell line	Rel. density[1]
A-375 parental	1.00
A-375-i-LB-U-mCherry	1.07
A-375-i-LB-U-mKate2	1.06

A-375 samples			
Cell line	Rel. density[1]	Adj. density[2]	Difference [%][3]
A-375 parental	1.00	1.00	
A-375-i-LB-U-mCherry	1.04	0.98	2.23
A-375-i-LB-U-mKate2	0.97	0.92	8.00

B

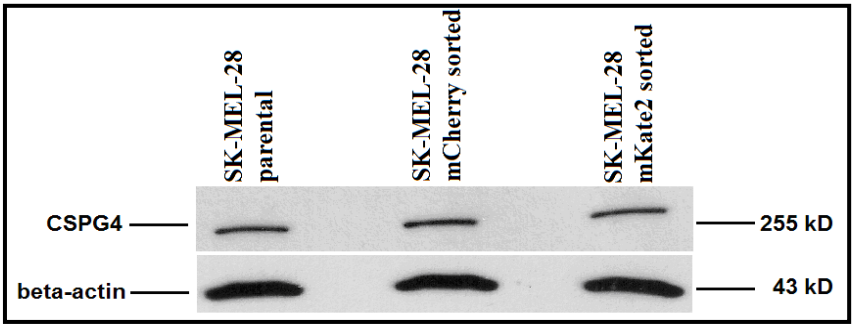

β-actin loading control	
Cell line	Rel. density[1]
SK-MEL-28 parental	1.00
SK-MEL-28-i-LB-U-mCherry sorted	1.02
SK-MEL-28-i-LB-U-mKate2 sorted	0.99

SK-MEL-28 samples			
Cell line	Rel. density[1]	Adj. density[2]	Difference [%][3]
SK-MEL-28 parental	1.00	1.00	
SK-MEL-28-i-LB-U-mCherry sorted	1.05	1.03	3.37
SK-MEL-28-i-LB-U-mKate2 sorted	0.96	0.97	3.38

C

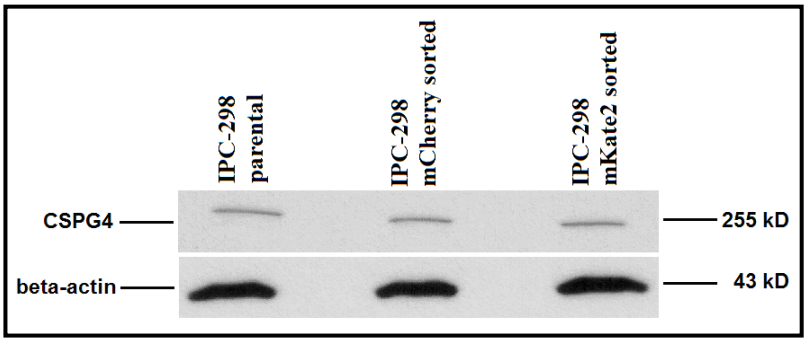

β-actin loading control	
Cell line	Rel. density[1]
IPC-298 parental	1.00
IPC-298-i-LB-U-mCherry sorted	0.95
IPC-298-i-LB-U-mKate2 sorted	1.08

IPC-298 samples			
Cell line	Rel. density[1]	Adj. density[2]	Difference [%][3]
IPC-298 parental	1.00	1.00	
IPC-298-i-LB-U-mCherry sorted	0.91	0.95	4.57
IPC-298-i-LB-U-mKate2 sorted	1.02	0.94	5.87

[1] Relative density = Percentage of infected cells divided by percentage of parental cells.
[2] Adjusted density = Relative Density of samples divided by corresponding relative density of loading controls.
[3] Difference [%] = Adjusted density of parental sample subtracted by each adjusted density value given by the infected cell samples x 100.

Figure 10. Level of CSPG4-expression on parental and transduced melanoma cells. After Western blotting and densitometric analysis of the bands, transduced A-375, SK-MEL-28 and IPC-298 cells revealed only marginal differences in amount of CSPG4-expression compared to their parental cell lines. **A.** A-375 cells showed the brightest bands followed by SK-MEL-28 cells shown in **B. C.** IPC-298 cells revealed the weakest bands compared to the other melanoma cell lines.

5.6 r28M-mediated *in vitro* cell killing

To test the killing capability of the bispecific single-chain antibody r28M on parental as well as on *mCherry*- and *mKate2*-transduced melanoma cells, a WST-1 cell viability assay was performed like explained in the Methods section. Two antibody sub-forms were tested: When applied in a concentration of 1000 ng per ml mix of PBMCs and tumour cells, the monomeric sub-form of the r28M antibody induced about 60 % killing of parental as well as transduced A-375 cells (Figure

11.A). Under the same conditions, 40 % cell killing of parental and transduced SK-MEL-28 cells was observed (Figure 11.B). Cell viability assays for the IPC-298 cells did not reveal interpretable data, which was the reason why those cells were excluded from the projected *in vivo* experiments.

When the dimeric sub-form of the r28M was tested, 90 to 95 % of parental as well as *mKate2*-transduced cells were killed (Figure 12). The A-375 cells transduced with *mCherry* were also killed to a high extend (up to 80 %, as shown in Figure 12). In all three samples no significant difference in killing was observed with the three different antibody concentrations of 50, 500 and 5000 ng/ml. We obtained similar data when another isolation product of the r28M dimer was tested under the same conditions (data not shown). As expected, no killing of tumour cells of the controls (tumour cells incubated with r28M alone and tumour cells with PBMCs alone) was observed.

Thus, we could show that the r28M antibody is able to induce effective killing of parental and *mCherry*- or *mKate2*-transduced A-375 cells, if it is applied in its dimeric form *in vitro*.

A

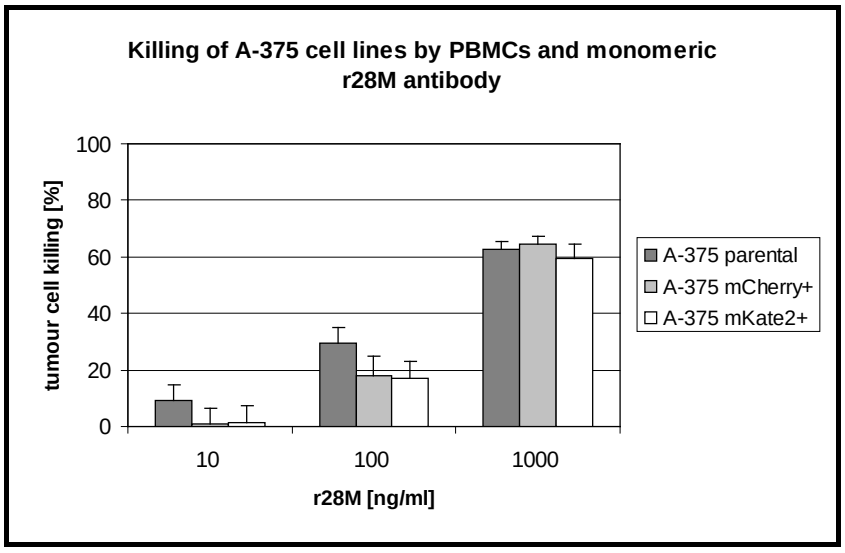

B

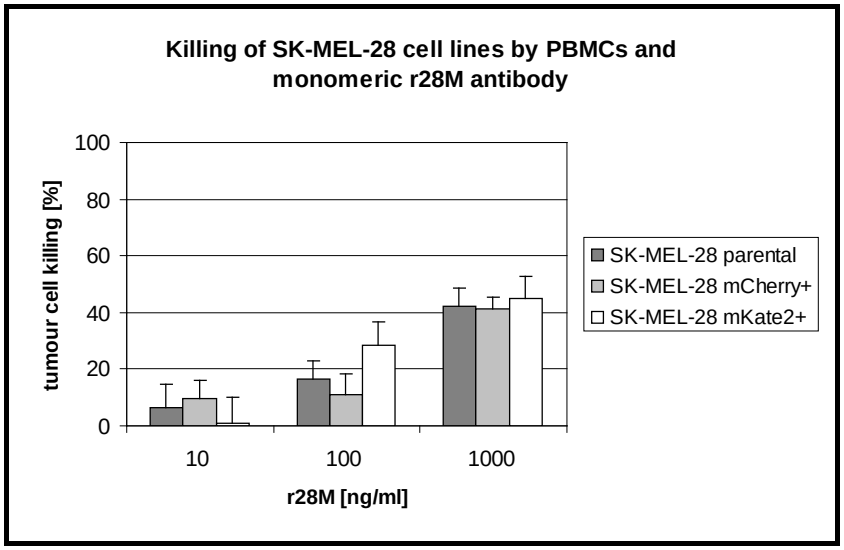

Figure 11. Killing of melanoma cell lines by PBMCs and monomeric r28M. The results shown here are representative for 3 sets of data. Each sample was measured in quadruplets; error bars represent their standard deviation. **A.** About 60 % of A-375 cells revealed to be killed with an antibody concentration of 1000 ng/ml. **B.** About 40 % of SK-MEL-28 cells were killed under the same conditions.

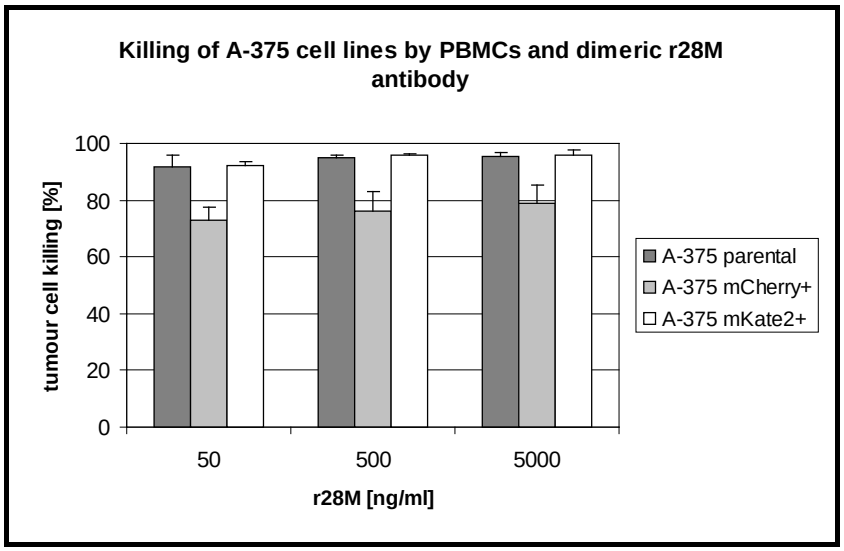

Figure 12. Killing of A-375 cell lines by PBMCs and dimeric r28M. The results shown here are representative for 3 sets of data. Each sample was measured in quadruplets; error bars represent their standard deviation. Almost all parental as well as *mKate2*-transduced A-375 cells were killed when the dimeric r28M antibody was used in three different concentrations. About 73 to 80 % of *mCherry*-transduced A-375 cells revealed to be killed under the same conditions.

5.7 Non-invasive visualisation of tumours in mice

To find out if the transduced cells are able to produce tumours in immune-deficient mice and if these tumours are detectable via IVIS, mCherry- and mKate2-positive A-375 cells were injected sub-cutaneously or directly into the brains of immune-deficient mice.

Mice bearing sc. tumours were visualised by IVIS in order to test the applicability of the machine (Figure 13, left mouse). To see if the tumours emerged by the transduced cells were detectable also through skull and skin, A-375 cells transduced with the gene for mCherry were injected into the brains of NSG-mice. Mice bearing these A-375-mCherry tumours showed rapid disease progression. After 20 days the tumours showed a size of approximately 5-8 mm, whereupon the mice were killed and visualised (Figure 13, right mouse).

Figure 13. Visualisation of tumours in immune-deficient mice. Left mouse: mKate2- (left), as well as mCherry-positive (right) tumours were detectable through the skin of a nude mouse. **Right mouse:** Also, brain tumours arisen by injection of mCherry-transduced A-375 cells were clearly detectable through skull and skin of NSG mice.

Thus, the transduced cells had the capability to form tumours after injection into immune-deficient mice. Moreover, these tumours could be detected non-invasively through skull and skin.

6 DISCUSSION

Malignant melanoma is one of the most deadly human cancers occurring worldwide.[78] Patients suffering from this disease show only poor survival rates due to lack of effective therapy for metastatic progression.[79] Therefore, it is of high importance to monitor the treatment efficiency of therapeutic agents by non-invasive visualisation methods.

Our aim was to generate human melanoma cell lines that stably express the red fluorescence proteins mCherry or mKate2 for visualisation of tumours in living mice. Moreover, we tested the killing potential of the bispecific single-chain antibody r28M on these tumour cells *in vitro*.

This research will provide the basis for the evaluation of the therapeutic effect of the r28M antibody as a part of a preclinical *in vivo* experiment.

When we estimated transduction rates and stability of RFP-expression within a transduced cell line, A-375 cells revealed to stably express the respective fluorescent proteins for over five months after antibiotic selection (Figure 6.A). In contrast, we observed insufficient numbers of RFP-expressing cells and/or unstable RFP-expression in transduced SK-MEL-28 and IPC-298 cells (data not shown). The reason for the low numbers of RFP-expressing cells as well as their decrease is difficult to explain. However, the following reasons can be taken into consideration: i) toxicity of the transgene, ii) promoter inactivation and iii) site of transgene integration into the host's genome.

After antibiotic selection of infected cells, similar numbers of colonies were obtained among the cell lines, which indicate similar infectivity of these cells. However, in SK-MEL-28 and IPC-298 cells we observed lower numbers of RFP-expressing cells as compared to the A-375 cells. We can speculate that suppression of transgene expression, as seen in the transduced SK-MEL-28 and IPC-298 cells, may be the result of transgene toxicity. Toxicity can occur due to high concentrations of the foreign proteins (e.g. fluorophores) caused by high transgene copy number or by aggregation of inaccurately localized fluorescence proteins.[80,81] It was observed that fluorescent proteins can be enriched in

lysosomes, which resulted in larger and maybe cytotoxic agglomerations.[80,82] For example, visible precipitates were detected in the cytosol, if the non-fused and monomeric version of RFP1 was transfected into HeLa cells.[82] In general, mCherry and mKate2 are reported to be low-toxic.[49,56,80] In 2008 Strack et al. compared the expression of mEGFP to the expression of various RFPs in lentivirally transduced HeLa cells.[83] For cells transduced with Ds-Red-Express, DsRed-Monomer, TagRFP, TurboRFP as well as mCherry, they observed a massive drop of average fluorescence intensities at day 10, which they explained by the loss of the most highly expressing cells after transduction.[83] This interpretation was further supported by the observation of a substantial drop of percentages of viable fluorescent cells transduced with these genes between day 3 and day 10 after infection.[83] For some RFPs (DsRed-Monomer, TagRFP and TurboRFP) they observed few fluorescent cells even at day 3, indicating cytotoxicity at early stages of expression.[83]

We can speculate that this might have also been the case for the *mKate2*-transduced SK-MEL-28 and IPC-298 melanoma cells, indicated by the low, but stable numbers of fluorescent cells directly after blasticidin selection. In contrast, no such effect was observed in *mKate2*-transduced A-375 cells, indicating that this effect may only occur when specific cell-RFP-combinations are used.

Another reason for the low and/or declining number of RFP-expressing cells observed after lentiviral transduction may be silencing of the transgene via inactivation of its promoter by epigenetic regulation. *De novo* methylation of transcriptional regulatory sequences or coding sequences is suggested to play an important role in the inactivation of exogenous genes and might function as a protective reaction against intrusion by foreign genetic materials.[84,85] Several viral promoters including the human cytomegalovirus immediate early promoter/enhancer (CMV-IEPE) or the Simian virus 40 (SV40) enhancer and early promoter were reported to have undergone transcriptional inactivation in several tissues including the brain.[86,87,88]

The transgenes used here were driven by a eukaryotic Ubiquitin C (UbC) promoter, which was established to improve the longevity of transgene expression.[87] Ubiquitin structures are highly conserved during evolution

whereupon the ubiquitin system is involved in many important cellular mechanisms including cell cycle, DNA repair and transcriptional regulation.[86] Therefore, this promoter may be more resistant to inactivating factors, and thus may overcome repression.[89] Previous studies have shown that transfection/transduction using the constitutive human UbC promoter to drive the transgene lead to prolonged high-level, ubiquitous expression of exogenous genes in various cell lines, transgenic mice and when incorporated into pDNA-vectors.[86]

Nevertheless, it was reported that inactivation might also happen to the UbC promoter in mice brain cells *in vivo*[90], indicating that this cellular promoter is not immune to inactivation through epigenetic regulation mechanisms. In 2012 Ngai et al. compared two types of lentiviral vectors carrying the *GFP* gene, one driven by a UbC promoter and the other by a CMV promoter in murine embryonic carcinoma cells.[91] They observed an about 2-folds higher GFP-expression of the cells when the *GFP* gene was driven by the CMV promoter compared to the expression under the UbC promoter 2 days as well as 14 days post-transduction and speculated that transgene silencing was caused by DNA methylation at the CpG sites in the promoter region.[91]

Suppressed transgene expression is also reported to occur if other internal housekeeping gene promoters are used. Kuriyama et al. observed that a transgene in retrovirally transduced mouse embryo fibroblasts was extensively or completely methylated if the gene was driven by an albumin gene promoter.[84] Thus, they concluded that the expression of the retrovirally transduced transgene may not persist *in vivo* even if the gene is driven by an internal housekeeping gene promoter.[84]

Alternatively, a promoter that is selectively expressed in melanocytes and melanomas (e.g. tyrosinase promoter) may help to overcome transcriptional inactivation caused by promoter inactivation. Nevertheless, the optimal combination of promoter and fluorescent transgenes must be evaluated for each new experiment.[92]

Moreover, the site of integration could have substantial effects on transgene expression, reaching from decrease in expression to complete silencing.[93] If a transgene integrates into inactive heterochromatin, its expression can be

suppressed or even completely silenced. Transgene integration by viral vectors was long reported to have happened randomly.[94,95] In 2007 integration sites of retro- and lentiviral vectors were mapped in CD34+ hematopoietic stem cells.[95] The authors identified hot spots of integration for retroviral and lentiviral vectors, whereupon RV but not LV hot spots were highly enriched in host genes.[95] These findings indicated that transgene integration by retroviral vectors favours promoter and enhancer regions, whereas the chance of random integration throughout the entire gene persists to be high in case of lentiviral vectors.[96] We assume that it is not likely that the site of integration is the reason for transgene silencing in the case of our *mCherry*- or *mKate2*-transduced SK-MEL-28 and IPC-298 cells, because only total populations were analysed in our studies.

Due to the low and/or unstable expression of the RFPs in *mCherry*- or *mKate2*-transduced SK-MEL-28 and IPC-298 cells transduced with the genes for mCherry or mKate2, these cells were sorted according to their RFP-expression, which resulted in more than 90 % of these cell lines stably expressing the respective fluorescent protein over several weeks (Figure 6.B and 6.C). Sorted *mKate2*-transduced IPC-298 cell line showed a tendency to lose RFP-expressing cells over time, starting at day 90. Nevertheless, a time period of 90 days is sufficient for the further planned visualisation experiments.

Moreover, our data revealed that each *mCherry*-transduced melanoma cell line showed higher brightness compared to the *mKate2*-transduced cell lines, regardless of which selection method was used. These observations form a contrast to previous findings in which mKate2 was reported to be about two times brighter than mCherry, when measured in relation to mEGFP.[51,56] We detected the difference in brightness not only by means of flow cytometry (not shown), but also when cells were monitored by UV-microscopy (Figure 7.A.2, B.2, C.2, D.2, E.2, F.2).

Regardless of the obstacles mentioned we were able to produce A-375, SK-MEL-28 and IPC-298 melanoma cell lines stably expressing mCherry or mKate2.

According to published literature data, A-375 cells as well as SK-MEL-28 cells are tumourigenic when injected into immune-compromised mice. [97-100] However, transgenes can alter the growth behaviour of transduced cells[59,101], which might be

reflected in tumour engraftment in animal models. Changes in growth behaviour may result not only in loss of, but also in increase of tumorigenicity, thus making the transduced cells unsuitable for long-term visualisation experiments *in vivo*. Therefore it is beneficial to inject cells with similar growth kinetics to those of the parental cells.

Such growth defects are reported to occur after transfection/transduction of cells with genes for fluorescent proteins.[59,101] In 2011 Verreault et al. sorted fluorescent cells according to the level of transgene expression and observed significant differences in growth rates between parental and *mCherry*- or *mKate2*-transduced U251MG glioblastoma cells.[59] The low mKate2-expressing U251MG cells showed growth rates comparable to those of the parental cells *in vitro*, as well as after inoculation in mice, whereas the very high, high and medium mKate2-expressing cells grew slower.[59] Also, the cell line highly expressing mCherry grew slower *in vitro*. As a result tumours emerged from those cells were no longer detectable on day 18.[59] The growth rates of the medium mCherry-expressing cells showed no significant differences to the ones of the parental line *in vivo*.[59] Verreault et al. speculated that these differences had occurred due to differences in gene copy number transduced into the cells, but also excluded copy number of being the only reason.[59] Therefore, they recommended testing of transduced cell populations for similarity in growth rates compared to parental cells.[59]

In addition, we have also experienced a significant decrease in growth kinetics of sorted U-87MG glioblastoma cells transduced with the gene for mKate2 *in vitro* as well as *in vivo* in our laboratory (data not shown). This prompted us to analyse the growth kinetics for our *mCherry*- or *mKate2*-transduced A-375, SK-MEL-28 and IPC-298 cells.

Thus, we excluded significant differences in proliferation rates between parental and transduced melanoma cells by comparing their growth rates and doubling times. Data revealed only minor differences (<7 % for each transduced cell line, as shown in Figure 8), whereupon the cells were considered for the upcoming *in vivo* visualisation experiments. The work of Verreault et al. differs from ours as we did not sort the transduced cells according to their brightness.

Thus, we worked with the total populations, which are likely to consist of a mix of low, medium and high RFP-expressing cells.

As described above, transduction of cells with lentiviral vectors may result in off-target effects on other genes since the integration can happen randomly. To exclude possible changes in CSPG4-expression we performed flow cytometric analysis and revealed the percentages of CSPG4-expressing cells among parental and transduced cell lines. We observed i) very high fractions of CSPG4-positive cells (~ 95-98 %) and ii) no significant differences in number of CSPG4-expressing cells between transduced and parental cells. Thus, our data are in accordance to previous reports in which high numbers of CSPG4-positive cells were detected within different melanoma cell types.[102,103] When we compared the data for the CSPG4-expression on A-375, SK-MEL-28 and IPC-298 cells to the literature, we found that the A-375 as well as the SK-MEL-28 cell lines were both reported to express CSPG4.[104-106] To our knowledge, no published data regarding the presence of CSPG4 on the melanoma cell line IPC-298 are available. Thus, we report the expression of this surface antigen on IPC-298 cells here for the first time.

Once we had confirmed that viral transduction had no impact on the number of CSPG4-expressing cells, we investigated whether or not transduction might have altered the amount of CSPG4-expression in the melanoma cells via semi-quantitative Western blot for CSPG4 on parental and *mCherry*- or *mKate2*-transduced A-375, SK-MEL-28 and IPC-298 cells. We observed comparable levels of CSPG4-expression between parental and transduced melanoma cells (Figure 10).

We speculate that the apparent difference in the amount of CSPG4-expression, as shown by the difference in brightness of the bands for CSPG4 between the different cell lines (A-375<SK-MEL-28<IPC-298) is due to higher number of CSPG4 molecules present in the A-375 compared to SK-MEL-28 and IPC-298 cells. This would be consistent with our flow cytometry data for CSPG4 in which the MFI emitted by the PE-conjugated secondary antibody was highest for A-375 cells (data not shown). In contrast, the SK-MEL-28 as well as the IPC-298 cells revealed only one-third of the MFI obtained from the A-375 cells (data not

shown). This is consistent with previous reports, in which CSPG4-expression was shown to be variable between various human melanoma cell lines.[104] Luo et al. investigated the CSPG4-expression of different human melanoma cell lines at the mRNA level by RT-PCR and at the protein level by Western blot.[104] Moreover they measured CSPG4 cell surface expression on these melanoma cells by flow cytometry.[104] Their data revealed that SK-MEL-5 cells expressed CSPG4 weakly at the mRNA level, whereas no protein expression was observed.[104] In contrast, the A-375 cells expressed CSPG4 both at the mRNA and at the protein level.[104] The authors demonstrated that CSPG4 promoter methylation plays a major role for the arising differences in CSPG4 expression between tested melanoma cell lines.[104] Thus, the differences in the brightness of the bands for CSPG4 as we obtained after Western blot may reflect different amount in CSPG4-expression caused by different methylation patterns of the CSPG4 promoter. Hence, we can speculate that the A-375 cell line provides more CSPG4 as targets for antibodies against this antigen compared to the SK-MEL-28 and IPC-298 cells. Therefore we assumed that the A-375 cells might be killed more effectively than the other cell lines when incubated with a mix of PBMCs and the r28M antibody. This assumption was substantiated in the subsequent proliferation assays, in which the A-375 cell line revealed to be killed to a higher extent than the others.

A more complex reason for the apparent difference in CSPG4-expression between the different melanoma cell lines as indicated by the differences in brightness of the bands may be caused by better binding capability of the purchased antibody for the CSPG4s on A-375 cells compared to the ones on SK-MEL-28 and IPC-298 cells. The core protein of CSPG4 is modified with chondroitin sulfate chains[107] (glycosaminoglycan chondroitin sulfates) that can hinder antibodies to bind the antigen. Therefore, Western blotting is often performed after digestion of the cell lysates with chondroitinase ABC[108-110] to provide access for the antibodies to CSPG4.

Nevertheless, the cell lines used here were tested for the brightness of the bands for CSPG4 by another group of our lab, whereupon no differences were detectable before and after lysate digestion with chondroitinase ABC (personal communication with Mag. rer. nat. Corinna Kern, Institute of Animal Breeding and

Genetics, University of Veterinary Medicine Vienna).

However, we showed that the relative amount of CSPG4-expression between transduced and parental cells is similar among each cell line. Therefore it can be concluded that viral transduction did not change CSPG4-expression in transduced melanoma cells. This indicates the suitability of the transduced cells developed here as targets for antibodies against this antigen. Therefore these cells were used to test the efficiency of the r28M antibody *in vitro*.

The r28M antibody proved to induce effective killing of tumour cells in cell viability assays *in vitro* as well as when applied in mice *in vivo*.[26,27] When this bispecific antibody was applied to a mixture of tumour cells and PBMCs it induced effective killing of the CSPG4-positive U87MG glioblastoma[26] and SK-MEL-63 melanoma cells[25], whereas it had no effect on viability of CSPG4-negative SKBr3[26] and T47D cells[27] *in vitro*. Moreover, r28M suppressed tumour growth, when applied together with freshly isolated PBMCs into nude mice.[26] These findings indicate the ability of the r28M antibody to induce cell-specific killing of the CSPG4-positive A-375, SK-MEL-28 and IPC-298 melanoma cells not only *in vitro*, but also *in vivo* in prospective experiments.

Due to the nature of the r28M-structure, purification and storage of the antibody can be challenging in the way to keep the same ratio between monomer and dimer[111]. Therefore, different purified products of the r28M were analysed for their tumour cell killing potential *in vitro*. As it has been shown for representative samples of each cell line in the Results section, we observed similar to what had been published for SK-MEL-63 cells by Grosse-Hovest et al.[25] We could show that the killing potential of the dimeric form of the r28M antibody, isolated and purified from cow blood in our laboratory, was superior to the killing potential of the monomeric form, even when the dimeric form was applied at lower concentrations (Figures 11.A-B and 12). Moreover we observed that out of the three melanoma cell lines tested the most effective killing was shown when A-375 cells or their transduced variants were used. We speculate that the abundant expression of the CSPG4 antigen on the cell surface is the reason for the effective killing, which is further indicated by Western blot (A-375 cells showed strongest bands, Figure 10.A) and flow cytometry data (A-375 cells had highest MFI, data not shown)

obtained, as explained above. In addition, the observed differences in killing efficiency between parental and transduced melanoma cells were marginal, which is also in accordance to our previously obtained Western blot and flow cytometry data, in which no differences in expression as for the numbers of positive cells as well as for the amount of protein present on the cells were detectable.

To analyse tumourigenic potential of *mCherry*- and *mKate2*-transduced A-375 cells *in vivo,* cells were injected subcutaneously into a nude mouse. Alternatively, the A-375 and SK-MEL-28 cells both transduced with *mCherry* were implanted into the brains of mice from a NOD.Cg-*Prkdc*^{scid} *Il2rg*^{tm1Wjl}/SzJ (NSG) mouse strain to obtain a brain metastases model of melanoma. Subsequently, we could visualise the emerged tumours via the IVIS, as demonstrated in Figure 13.

This model will provide the basis for monitoring the efficiency of the r28M antibody to induce killing of *mCherry*- or *mKate2*-transduced melanoma cells in prospective experiments, which was previously shown to work in U251MG glioblastoma cells.[59] In 2011 Verreault et al. were able to estimate tumour sizes of orthotopically implanted tumours emerged by *mCherry*- or *mKate2*-transduced U251MG cells with the Maestro multispectral fluorescent imaging system in Rag2M mice.[59] Based on these findings they could measure treatment efficiency of temozolomide (TMZ) as well.[59] Moreover, the authors monitored tumour growth over time in NOD.CB17-SCID mice bearing mKate2-tumours.[59] Thus, they demonstrated that tumour progression/regression and treatment efficacy can be monitored based on measurements of changes in fluorescence intensity from the brains of small animals inoculated with *mCherry*- or *mKate2*-transduced U251MG cells.[59]

7 SUMMARY AND CONCLUSION

It can be concluded that we have successfully generated human melanoma cells that stably express the fluorescence proteins mCherry and mKate2 for *in vivo* visualisation of tumours. The lentivirally transduced cells showed tumourigenicity *in vivo*, whereupon the signals generated by the fluorescent tumours could be detected and measured through skin and skull via IVIS.

In prospective experiments the other cell lines generated here will also be tested in NSG mice and these findings will be used to monitor the treatment efficiency of the r28M antibody in humanized mice.

Non-invasive visualisation methods as facilitated with the use of red fluorescence proteins in whole-body imaging in mice help to reduce the numbers of animals needed for experimental testing. Instead of killing a large number of animals to be able to monitor tumour growth and efficiency of treatment attempts over time in histological studies, the same animal can be measured regularly if the tumour is detectable via IVIS.

Moreover the use of non-invasive imaging helps monitoring tumour development prior to any appreciable changes in health status of the animals. This reduces the number of animals that die as a result of tumour formation prior euthanasia.[59]

Most importantly non-invasive real-time fluorescence imaging techniques will facilitate the discoveries and testing of candidate antitumour agents for inhibition of cancer growth and progression.

8 REFERENCES

1. Singh AD, Bergman L, and Seregard S. Uveal malignant melanoma: epidemiologic aspects. *Essentials of Ophthalmic Oncology* (2009); 78-80. ISBN 978-1-55642-9170; Slack Incorporated.

2. Blecker D, Abraham S, Furth EE, and Kochman ML. Melanoma in the gastrointestinal tract. *Am J Gastroenterol* (1999); 94: 3427–3433; doi: 10.1111/j.1572-0241.1999.01604.x.

3. American Cancer Society. Cancer Facts & Figures 2012. Atlanta: American Cancer Society (2012).

4. Jerant AF, Johnson JT, Sheridan CD and Caffrey TJ. Early detection and treatment of skin cancer. *Am Fam Physician* (2000); 62(2): 357-368.

5. Garbe C and Leiter U. Melanoma epidemiology and trends. *Clin Dermatol* (2009); 27(1): 3-9; doi: 10.1016/j.clindermatol.2008.09.001.

6. Field JK. Oncogenes and tumour-suppressor genes in squamous cell carcinoma of the head and neck. *Eur J Cancer B Oral Oncol* (1992); 28B(1): 67-76.

7. Clark WH Jr, Elder DE, Guerry D 4th, Epstein MN, Greene MH, and Van Horn M. A study of tumor progression: the precursor lesions of superficial spreading and nodular melanoma. *Hum Pathol* (1984); 15(12): 1147-65.

8. Jandus C, Speiser D, and Romero P. Recent advances and hurdles in melanoma immunotherapy. *Pigment Cell Melanoma Res* (2009); 22(6):711-23; doi: 10.1111/j.1755-148X.2009.00634.x.

9. Su DM, Zhang Q, Wang X, He P, Zhu YJ, Zhao J, et al. Two types of human malignant melanoma cell lines revealed by expression patterns of mitochondrial and survival-apoptosis genes: implications for malignant melanoma therapy. *Cancer Ther* (2009); 8(5): 1292–1304; doi: 10.1158/1535-7163.MCT-08-1030.

10. Villanueva J, Vultur A, Lee JT, Somasundaram R, Fukunaga-Kalabis M, Cipolla AK, et al. Acquired resistance to BRAF inhibitors mediated by a RAF kinase switch in melanoma can be overcome by cotargeting MEK and IGF-1R/PI3K. *Cancer Cell* (2010); 18(6): 683-95; doi: 10.1016/j.ccr.2010.11.023.

11. Soengas MS and Lowe SW. Apoptosis and melanoma chemoresistance. *Oncogene* (2003); 22(20): 3138-51.

12. Buzaid AC. Management of Metastatic Cutaneous Melanoma; *Oncology*; 18(11): 1443–1450; discussion 1457–1459.

13. Davar D, Tarhini A, and Kirkwood JM. Adjuvant therapy: melanoma. *J Skin Cancer* (2011); 2011:274382; doi: 10.1155/2011/274382.

14. Petrella T, Verma S, Spithoff K, Quirt I, McCready D and Melanoma Disease Site Group. Adjuvant interferon therapy for patients at high risk for recurrent melanoma: an updated systematic review and practice guideline. *Clin Oncol (R Coll Radiol)* (2012); 24(6): 413-23; doi: 10.1016/j.clon.2011.12.002.

15. Chapman PB, Hauschild A, Robert C, Haanen JB, Ascierto P, Larkin J. et al. Improved survival with vemurafenib in melanoma with BRAF V600E mutation. *N Engl J Med.* (2011); 364(26): 2507-16; doi: 10.1056/NEJMoa1103782.

16. Traynor K. Ipilimumab approved for metastatic melanoma. *J Health Syst Pharm* (2011); 68(9): 768; doi: 10.2146/news110025.

17. O'Day SJ, Hamid O, and Urba WJ. Targeting cytotoxic T-lymphocyte antigen-4 (CTLA-4): a novel strategy for the treatment of melanoma and other malignancies. *Cancer* (2007); 110(12): 2614-27; doi: 10.1002/cncr.23086.

18. O'Day SJ, Hodi FS, McDermott DF, Weber RW, Sosman JA, Haanen JB et al. A phase III, randomized, double-blind, multicenter study comparing monotherapy with ipilimumab or gp100 peptide vaccine and the combination in patients with previously treated, unresectable stage III or IV melanoma. *J Clin Oncol* (2010); 28: 18s.

19. Robert C, Thomas L, Bondarenko I, O'Day S, Weber J, Garbe C et al. Ipilimumab plus Dacarbazine for Previously Untreated Metastatic Melanoma. *N Engl J Med* (2011); 364: 2517-2526, doi: 10.1056/NEJMoa1104621.

20. Van Spriel AB, Van Ojik HH, and Van De Winkel JG. Immunotherapeutic perspective for bispecific antibodies. *Immunol Today* (2000); 21(8): 391-397*;* doi: 10.1016/S0167-5699(00)01659-5.

21. Segal DM, Weiner GJ, and Weiner LM. Bispecific antibodies in cancer therapy. *Curr Opin Immunol.* (1999); 11(5): 558-62.

22. Fanger MW, Morganelli PM, and Guyre PM. Bispecific antibodies. *Crit Rev Immunol* (1992); 12(3-4): 101-24.

23. Gruber M, Schodin BA, Wilson ER, and Kranz DM. Efficient tumor cell lysis mediated by a bispecific single chain antibody expressed in Escherichia coli. *J Immunol* (1994); 152(11) :5368-74.

24. De Jonge J, Heirman C, de Veerman M, Van Meirvenne S, Moser M, Leo O et al. In vivo retargeting of T cell effector function by recombinant bispecific single chain Fv (anti-CD3 x anti-idiotype) induces long-term survival in the murine BCL1 lymphoma model. *J Immunol* (1998); 161(3): 1454-61.

25. Grosse-Hovest L, Hartlapp I, Marwan W, Brem G, Rammensee HG, and Jung G. A recombinant bispecific single-chain antibody induces targeted, supra-agonistic CD28-stimulation and tumor cell killing. *Eur J Immunol* (2003); 33(5): 1334-40; doi: 10.1002/eji.200323322.

26. Grosse-Hovest L, Wick W, Minoia R, Weller M, Rammensee HG, Brem G, and Jung G. Supraagonistic, bispecific single-chain antibody purified from the serum of cloned, transgenic cows induces T-cell-mediated killing of glioblastoma cells in vitro and in vivo. *Int J Cancer* (2005); 117(6): 1060-4; doi: 10.1002/ijc.21294.

27. Grosse-Hovest L, Müller S, Minoia R, Wolf E, Zakhartchenko V, Wenigerkind H, et al. Cloned transgenic farm animals produce a bispecific antibody for T cell-mediated

tumor cell killing. *Proc Natl Acad Sci U S A.* (2004); 101(18): 6858-63; doi: 10.1073/pnas.0308487101.

28. Otz T, Grosse-Hovest L, Hofmann M, Rammensee HG, and Jung G. A bispecific single-chain antibody that mediates target cell-restricted, supra-agonistic CD28 stimulation and killing of lymphoma cells. *Leukemia* (2009); 23(1):71-7; doi: 10.1038/leu.2008.271.

29. Europäisches Patentamt. Europäische Patentschrift EP 1 444 268 B1; (2007).

30. Suntharalingam G, Perry MR, Ward S, Brett SJ, Castello-Cortes A, Brunner MD, et al. Cytokine storm in a phase 1 trial of the anti-CD28 monoclonal antibody TGN1412. *N Engl J Med* (2006) ;355(10): 1018-28.

31. Patrick Chames and Daniel Baty. Bispecific antibodies for cancer therapy. The light at the end of the tunnel? *MAbs* (2009); 1(6): 539–547.

32. Price MA, Colvin Wanshura LE, Yang J, Carlson J, Xiang B, Li G, et al. CSPG4, a potential therapeutic target, facilitates malignant progression of melanoma. *Pigment Cell Melanoma Res* (2011); 24(6): 1148-57; doi: 10.1111/j.1755-148X.2011.00929.x.

33. Wilson BS, Imai K, Natali PG, and Ferrone S. Distribution and molecular characterization of a cell-surface and a cytoplasmic antigen detectable in human melanoma cells with monoclonal antibodies. *Int J Cancer* (1981); 28(3): 293-300.

34. R and Mihich E. Eighteenth annual pezcoller symposium: tumor microenvironment and heterotypic interactions. *Cancer Res* (2006); 66(24): 11550-3; doi: 10.1158/0008-5472.CAN-06-3149.

35. Schlingemann RO, Rietveld FJ, de Waal RM, Ferrone S, and Ruiter DJ. Expression of the high molecular weight melanoma-associated antigen by pericytes during angiogenesis in tumors and in healing wounds. *Am J Pathol* (1990); 136(6): 1393-405.

36. Huang FJ, You WK, Bonaldo P, Seyfried TN, Pasquale EB, and Stallcup WB. Pericyte deficiencies lead to aberrant tumor vascularizaton in the brain of the NG2 null mouse. *Dev Biol* (2010); 344(2): 1035-46; doi: 10.1016/j.ydbio.2010.06.023.

37. Ghali L, Wong ST, Tidman N, Quinn A, Philpott MP, and Leigh IM. Epidermal and hair follicle progenitor cells express melanoma-associated chondroitin sulfate proteoglycan core protein. *J Invest Dermatol* (2004); 122(2): 433-42; doi: 10.1046/j.0022-202X.2004.22207.x.

38. Trotter J, Karram K, and Nishiyama A. NG2 cells: Properties, progeny and origin. *Brain Res Rev* (2010); 63(1-2): 72-82; doi: 10.1016/j.brainresrev.2009.12.006.

39. Yang J, Price MA, Li GY, Bar-Eli M, Salgia R, Jagedeeswaran R, et al. Melanoma proteoglycan modifies gene expression to stimulate tumor cell motility, growth, and epithelial-to-mesenchymal transition. *Cancer Res* (2009); 69(19): 7538-47; doi: 10.1158/0008-5472.CAN-08-4626.

40. Wang X, Osada T, Wang Y, Yu L, Sakakura K, Katayama A, et al. CSPG4 protein as a new target for the antibody-based immunotherapy of triple-negative breast cancer. *J Natl Cancer Inst* (2010); 102(19): 1496-512; doi: 10.1093/jnci/djq343.

41. Wang J, Svendsen A, Kmiecik J, Immervoll H, Skaftnesmo KO, Planagumà J, et al. Targeting the NG2/CSPG4 proteoglycan retards tumour growth and angiogenesis in preclinical models of GBM and melanoma. *PLoS One* (2011); 6(7): e23062; doi: 10.1371/journal.pone.0023062.

42. Cui K, Xu X, Zhao H, and Wong ST. A quantitative study of factors affecting in vivo bioluminescence imaging. *Luminescence* (2008); 23(5): 292-5; doi: 10.1002/bio.1032.

43. Honigman A, Zeira E, Ohana P, Abramovitz R, Tavor E, Bar I, et al. Imaging transgene expression in live animals. *Mol Ther* (2001); 4(3): 239-49.

44. Gillies RJ, Schornack PA, Secomb TW, and Raghunand N. Causes and effects of heterogeneous perfusion in tumors. *Neoplasia* (1999); 1(3): 197-207.

45. Lee KH, Byun SS, Paik JY, Lee SY, Song SH, Choe YS, et al. Cell uptake and tissue distribution of radioiodine labelled D-luciferin: implications for luciferase based gene imaging. *Nucl Med Commun* (2003); 24(9): 1003-9.

46. Monya Baker. A broader palette for luciferase. *Nature Methods* (2012); 9, 225; doi: 10.1038/nmeth.1919.

47. Hoffman RM. Multiple uses of fluorescent proteins to visualize cancer in vivo. *Nat Rev Cancer* (2005); 5(10): 796-806; doi:10.1038/nrc1717.

48. Fink D, Wohrer S, Pfeffer M, Tombe T, Ong CJ, and Sorensen PH. Ubiquitous expression of the monomeric red fluorescent protein mCherry in transgenic mice. *Genesis* (2010); 48(12): 723-9; doi: 10.1002/dvg.20677.

49. Shcherbo D, Merzlyak EM, Chepurnykh TV, Fradkov AF, Ermakova GV, Solovieva EA et al. Bright far-red fluorescent protein for whole-body imaging. *Nat Methods* (2007); 4(9): 741-6; doi:10.1038/nmeth1083.

50. Hintersdorfer P and Van Antoine O. Handbook of Single-Molecule Biophysics. *Springer* (2009); ISBN 978-0-387-76496-2; doi: 10.1007/978-0-387-76497-9.

51. Shcherbo D, Murphy CS, Ermakova GV, Solovieva EA, Chepurnykh TV, Shcheglov AS, et al. Far-red fluorescent tags for protein imaging in living tissues. *Biochem J* (2009); 418(3): 567-74; doi: 10.1042/BJ20081949.

52. Yang M, Baranov E, Jiang P, Sun F-X, Li X-M, Li L, et al. Whole-body optical imaging of green fluorescent protein-expressing tumors and metastases. *PNAS* (2000); 97(3): 1206-1211; doi: 10.1073/pnas.97.3.1206.

53. Katz MH, Takimoto S, Spivack D, Moossa AR, Hoffman RM and Bouvet M. A novel red fluorescent protein orthotopic pancreatic cancer model for the preclinical evaluation of chemotherapeutics. *J Surgical Res* (2003); 113: 151-160; doi: 10.1016/S0022-4804(03)00234-8.

54. Katz MH, Bouvet M, Takimoto S, Spivack D, Moossa AR, and Hoffman RM.. Selective antimetastatic activity of cytosine analog CS-682 in a red fluorescent protein orthotopic model of pancreatic cancer. *Cancer Res* (2003); 63(17): 5521-5.

55. Shu X, Shaner NC, Yarbrough CA, Tsien RY, and Remington SJ. Novel chromophores and buried charges control color in mFruits. *Biochemistry* (2006); 45(32): 9639-47.

56. Shaner NC, Campbell RE, Steinbach PA, Giepmans BN, Palmer AE, and Tsien RY. Improved monomeric red, orange and yellow fluorescent proteins derived from Discosoma sp. red fluorescent protein. *Nat Biotechnol* (2004); 22(12): 1567-72; doi: 10.1038/nbt1037.

57. Lagendijk EL, Validov S, Lamers GE, de Weert S, and Bloemberg GV. Genetic tools for tagging Gram-negative bacteria with mCherry for visualization in vitro and in natural habitats, biofilm and pathogenicity studies. *FEMS Microbiol Lett* (2010); 305(1): 81-90; doi: 10.1111/j.1574-6968.2010.01916.x.

58. Shaner NC, Steinbach PA, and Tsien RY. A guide to choosing fluorescent proteins. *Nat Methods* (2005); 2(12): 905-9; doi: 10.1038/nmeth819.

59. Verreault M, Strutt D, Masin D, Fink D, Gill R, and Bally MB. Development of glioblastoma cell lines expressing red fluorescence for non-invasive live imaging of intracranial tumors. *Anticancer Res* (2011); 31(6): 2161-71.

60. Douglas KL. Toward development of artificial viruses for gene therapy: a comparative evaluation of viral and non-viral transfection. *Biotechnol Prog* (2008); 24(4): 871-83. doi: 10.1021/bp070319o.

61. Djurovic S, Iversen N, Jeansson S, Hoover F, and Christensen G. Comparison of nonviral transfection and adeno-associated viral transduction on cardiomyocytes. *Mol Biotechnol* (2004); 28(1): 21-32; doi: 10.1385/MB:28:1:21.

62. Sakuma T, Barry MA, and Ikeda Y. Lentiviral vectors: basic to translational. *Biochem J* (2012); 443(3): 603-18; doi: 10.1042/BJ20120146.

63. Lewis P, Hensel M, and Emerman M. Human immunodeficiency virus infection of cells arrested in the cell cycle. *EMBO J* (1992); 11(8): 3053-8.

64. Costin JM. Cytopathic mechanisms of HIV-1. *Virol J* (2007); 4:100; doi: 10.1186/1743-422X-4-100.

65. Blömer U, Naldini L, Kafri T, Trono D, Verma IM, and Gage FH. Highly efficient and sustained gene transfer in adult neurons with a lentivirus vector. *J Virol* (1997); 71(9): 6641-9.

66. Sirven A, Pflumio F, Zennou V, Titeux M, Vainchenker W, Coulombel L, et al. The human immunodeficiency virus type-1 central DNA flap is a crucial determinant for lentiviral vector nuclear import and gene transduction of human hematopoietic stem cells. *Blood* (2000); 96(13): 4103-10.

67. Ray P, De A, Min JJ, Tsien RY, and Gambhir SS. Imaging tri-fusion multimodality reporter gene expression in living subjects. *Cancer Res* (2004); 64(4): 1323-30; doi: 10.1158/0008-5472.CAN-03-1816.

68. Murakami T, Cardones AR, and Hwang ST. Chemokine receptors and melanoma metastasis. *J Dermatol Sci* (2004); 36(2): 71-8; doi: 10.1016/j.jdermsci.2004.03.002

69. Kehrli P. Epidemiology of brain metastases. *Neurochirurgie* (1999); 45(5): 357-63.

70. Nussbaum ES, Djalilian HR, Cho KH, and Hall WA. Brain metastases. Histology, multiplicity, surgery, and survival. *Cancer* (1996); 78(8): 1781-8.

71. Gabriele Schackert and Isaiah J. Fidler. Site-specific Metastasis of Mouse Melanomas and a Fibrosarcoma in the Brain or Meninges of Syngeneic Animals. *Cancer Res* (1988); 48: 3478-3484.

72. The Jackson Laboratory website. http://jaxmice.jax.org/research/immunology/005557-faq.html

73. Carreno BM, Garbow JR, Kolar GR, Jackson EN, Engelbach JA, Becker-Hapak M, et al. Immunodeficient mouse strains display marked variability in growth of human melanoma lung metastases. *Clin Cancer Res* (2009); 15(10): 3277-86; doi: 10.1158/1078-0432.CCR-08-2502.

74. Shultz LD, Lyons BL, Burzenski LM, Gott B, Chen X, Chaleff S, et al. Human lymphoid and myeloid cell development in NOD/LtSz-scid IL2R gamma null mice engrafted with mobilized human hemopoietic stem cells. *J Immunol* (2005); 174(10): 6477-89.

75. Quintana E, Piskounova E, Shackleton M, Weinberg D, Eskiocak U, Fullen DR, et al. Human melanoma metastasis in NSG mice correlates with clinical outcome in patients. *Sci Transl Med* (2012); 4(159): 159ra149; doi: 10.1126/scitranslmed.3004599.

76. Sarry JE, Murphy K, Perry R, Sanchez PV, Secreto A, Keefer C, et al. Human acute myelogenous leukemia stem cells are rare and heterogeneous when assayed in NOD/SCID/IL2Rγc-deficient mice. *J Clin Invest* (2011); 121(1): 384-95; doi: 10.1172/JCI41495.

77. Quintana E, Shackleton M, Sabel MS, Fullen DR, Johnson TM, and Morrison SJ. Efficient tumour formation by single human melanoma cells. *Nature* (2008); 456 (7222): 593-8; doi: 10.1038/nature07567.

78. Dahl C and Guldberg P. The genome and epigenome of malignant melanoma. *APMIS* (2007); 115 (10): 1161-76; doi: 10.1111/j.16000463.2007.apm_855.xml.x.

79. Madhunapantula SV, Sharma A, Robertson GP. PRAS40 deregulates apoptosis in malignant melanoma. *Cancer Res* (2007); 67(8): 3626-36, doi: 10.1158/0008-5472.CAN-06-4234.

80. Chudakov DM, Matz MV, Lukyanov S, and Lukyanov KA. Fluorescent Proteins and Their Applications in Imaging Living Cells and Tissues. *Physiol Rev* (2010); 90(3): 1103-63; doi: 10.1152/physrev.00038.2009.

81. Yanushevich YG, Staroverov DB, Savitsky AP, Fradkov AF, Gurskaya NG, Bulina ME, et al. A strategy for the generation of non-aggregating mutants of Anthozoa fluorescent proteins. *FEBS Lett* (2002); 511(1-3): 11-4; doi: 10.1016/S0014-5793(01)03263-X.

82. Katayama H, Yamamoto A, Mizushima N, Yoshimori T, and Miyawaki A. GFP-like proteins stably accumulate in lysosomes. *Cell Struct Funct* (2008); 33(1) :1-12.

83. Strack RL, Strongin DE, Bhattacharyya D, Tao W, Berman A, Broxmeyer HE, et al. A noncytotoxic DsRed variant for whole-cell labeling*. Nat Methods* (2008); 5(11): 955-7; doi: 10.1038/nmeth.1264.

84. Kuriyama S, Sakamoto T, Kikukawa M, Nakatani T, Toyokawa Y, Tsujinoue H, et al. Expression of a retrovirally transduced gene under control of an internal housekeeping gene promoter does not persist due to methylation and is restored partially by 5-azacytidine treatment. *Gene Ther* (1998); 5(10): 1299-305.

85. Doerfler W. Patterns of DNA methylation--evolutionary vestiges of foreign DNA inactivation as a host defense mechanism. A proposal. *Biol Chem Hoppe Seyler* (1991); 372(8): 557-64.

86. Gazdhar A, Bilici M, Pierog J, Ayuni EL, Gugger M, Wetterwald A, et al. In vivo electroporation and ubiquitin promoter--a protocol for sustained gene expression in the lung. *J Gene Med* (2006); 8(7): 910-8; doi: 10.1002/jgm.911.

87. Papadakis ED, Nicklin SA, Baker AH, and White SJ. Promoters and control elements: designing expression cassettes for gene therapy. *Curr Gene Ther* (2004); 4(1): 89-113; doi: 10.2174/1566523044578077.

88. Fitzsimons HL, Bland RJ, and During MJ. Promoters and regulatory elements that improve adeno-associated virus transgene expression in the brain. *Methods* (2002); 28(2): 227-36. doi: 10.1016/S1046-2023(02)00227-X.

89. Habib N, Havlík R, Jiao L, Kiri A, Jensen S, Nicholls J, et al. Combination of Optison™ with ultrasound and electroporation increases albumin and thrompoietin transgene

expression whilst elongation factor promoter prolongs its duration. *Gene Therapy & Molecular Biol* (2004); 8(A),1-8.

90. Wilhelm F, Winkler U, Morawski M, Jäger C, Reinecke L, Rossner MJ, et al. The human ubiquitin C promoter drives selective expression in principal neurons in the brain of a transgenic mouse line. *Neurochem Int* (2011); 59(6): 976-80; doi: 10.1016/j.neuint.2011.07.008.

91. Ngai SC, Ramasamy R and Abdullah S. Production of Lentivirus Carrying Green fluorescent Protein with Different Promoters for in vitro Gene Transfer. *Pertanika J Sci & Technol* (2012); 20 (2): 269 – 281.

92. Jensen EC. Use of fluorescent probes: their effect on cell biology and limitations. *Anat Rec (Hoboken)* (2012); 295(12): 2031-6; doi: 10.1002/ar.22602.

93. Vasileva A, Jessberger R. Precise hit: adeno-associated virus in gene targeting. *Nat Rev Microbiol* (2005); 3(11): 837-47.

94. Ohbayashi F, Balamotis MA, Kishimoto A, Aizawa E, Diaz A, Hasty P, et al. Correction of chromosomal mutation and random integration in embryonic stem cells with helper-dependent adenoviral vectors. *Proc Natl Acad Sci U S A* (2005); 102(38): 13628-33.

95. Cattoglio C, Facchini G, Sartori D, Antonelli A, Miccio A, Cassani B, et al. Hot spots of retroviral integration in human CD34+ hematopoietic cells. *Blood* (2007); 110(6): 1770-8; doi: 10.1182/blood-2007-01-068759.

96. Yi Y, Noh MJ, and Lee KH. Current advances in retroviral gene therapy. *Curr Gene Ther* (2011); 11(3): 218-28; doi: 10.2174/156652311795684740.

97. Price JE, Polyzos A, Zhang RD, and Daniels LM. Tumorigenicity and metastasis of human breast carcinoma cell lines in nude mice. *Cancer Res* (1990); 50(3): 717-21.

98. Graells J, Vinyals A, Figueras A, Llorens A, Moreno A, Marcoval J, et al. Overproduction of VEGF concomitantly expressed with its receptors promotes growth

and survival of melanoma cells through MAPK and PI3K signaling. *J Invest Dermatol* (2004); 123(6): 1151-61; doi: 10.1111/j.0022-202X.2004.23460.x.

99. Huang S, DeGuzman A, Bucana CD, and Fidler IJ. Nuclear factor-kappaB activity correlates with growth, angiogenesis, and metastasis of human melanoma cells in nude mice. *Clin Cancer Res* (2000); 6(6): 2573-81.

100. Fogh J, Fogh JM, and Orfeo T. One hundred and twenty-seven cultured human tumor cell lines producing tumors in nude mice. *J Natl Cancer Inst* (1977); 59(1): 221-6.

101. Tao W, Evans BG, Yao J, Cooper S, Cornetta K, Ballas CB, et al. Enhanced green fluorescent protein is a nearly ideal long-term expression tracer for hematopoietic stem cells, whereas DsRed-express fluorescent protein is not. *Stem Cells* (2007); 25(3): 670-8, doi: 10.1634/stemcells.2006-0553.

102. Nishi H, Inoue Y, Kageshita T, Takata M, and Ihn H. The expression of human high molecular weight melanoma-associated antigen in acral lentiginous melanoma. *Biosci Trends* (2010); 4(2): 86-9.

103. Campoli MR, Chang CC, Kageshita T, Wang X, McCarthy JB, and Ferrone S. Human high molecular weight-melanoma-associated antigen (HMW-MAA): a melanoma cell surface chondroitin sulfate proteoglycan (MSCP) with biological and clinical significance. *Crit Rev Immunol* (2004); 24(4): 267-96.

104. Luo W, Wang X, Kageshita T, Wakasugi S, Karpf AR, and Ferrone S. Regulation of high molecular weight-melanoma associated antigen (HMW-MAA) gene expression by promoter DNA methylation in human melanoma cells. *Oncogene* (2006); 25(20): 2873-84.

105. Wang X, Katayama A, Wang Y, Yu L, Favoino E, Sakakura K, et al. Functional characterization of an scFv-Fc antibody that immunotherapeutically targets the common cancer cell surface proteoglycan CSPG4. *Cancer Res* (2011); 71(24): 7410-22; doi: 10.1158/0008-5472.CAN-10-1134.

106. Yu L, Favoino E, Wang Y, Ma Y, Deng X, and Wang X. The CSPG4-specific monoclonal antibody enhances and prolongs the effects of the BRAF inhibitor in melanoma cells. *Immunol Res* (2011); 50(2-3): 294-302; doi: 10.1007/s12026-011-8232-z.

107. Yang J, Price MA, Li GY, Bar-Eli M, Salgia R, Jagedeeswaran R, et al. Melanoma proteoglycan modifies gene expression to stimulate tumor cell motility, growth, and epithelial-to-mesenchymal transition. *Cancer Res* (2009); 69(19): 7538-47; doi: 10.1158/0008-5472.CAN-08-4626.

108. Moransard M, Dann A, Staszewski O, Fontana A, Prinz M, and Suter T. NG2 expressed by macrophages and oligodendrocyte precursor cells is dispensable in experimental autoimmune encephalomyelitis. *Brain* (2011; 134(Pt 5): 1315-30; doi: 10.1093/brain/awr070.

109. Lin HW, Basu A, Druckman C, Cicchese M, Krady JK, and Levison SW. Astrogliosis is delayed in type 1 interleukin-1 receptor-null mice following a penetrating brain injury. *J Neuroinflammation* (2006); 3:15; doi: 10.1186/1742-2094-3-15.

110. Morgenstern DA, Asher RA, Naidu M, Carlstedt T, Levine JM, and Fawcett JW. Expression and glycanation of the NG2 proteoglycan in developing, adult, and damaged peripheral nerve. *Mol Cell Neurosci* (2003); 24(3): 787-802; doi: 10.1016/S1044-7431(03)00245-8.

111. Arndt KM, Müller KM, and Plückthun A. Factors influencing the dimer to monomer transition of an antibody single-chain Fv fragment. *Biochemistry* (1998); 37(37): 12918-26.

112. Zaidi MR, Day CP, and Merlino G. From UVs to metastases: modeling melanoma initiation and progression in the mouse. *J Invest Dermatol* (2008); 128(10): 2381-91; doi: 10.1038/jid.2008.177.

„Ich habe mich bemüht, sämtliche Inhaber der Bildrechte ausfindig zu machen und ihre Zustimmung zur Verwendung der Bilder in dieser Arbeit eingeholt. Sollte dennoch eine Urheberrechtsverletzung bekannt werden, ersuche ich um Meldung bei mir.“

“I used my best endeavours to seek all claim holders of the pictures and obtain their permission to use their pictures in my thesis. Still, if any copyright infringement should emerge, please inform me.”

9 APPENDIX

9.1 Supplements

Supplement 1. Map of pLB-U-mCherry.

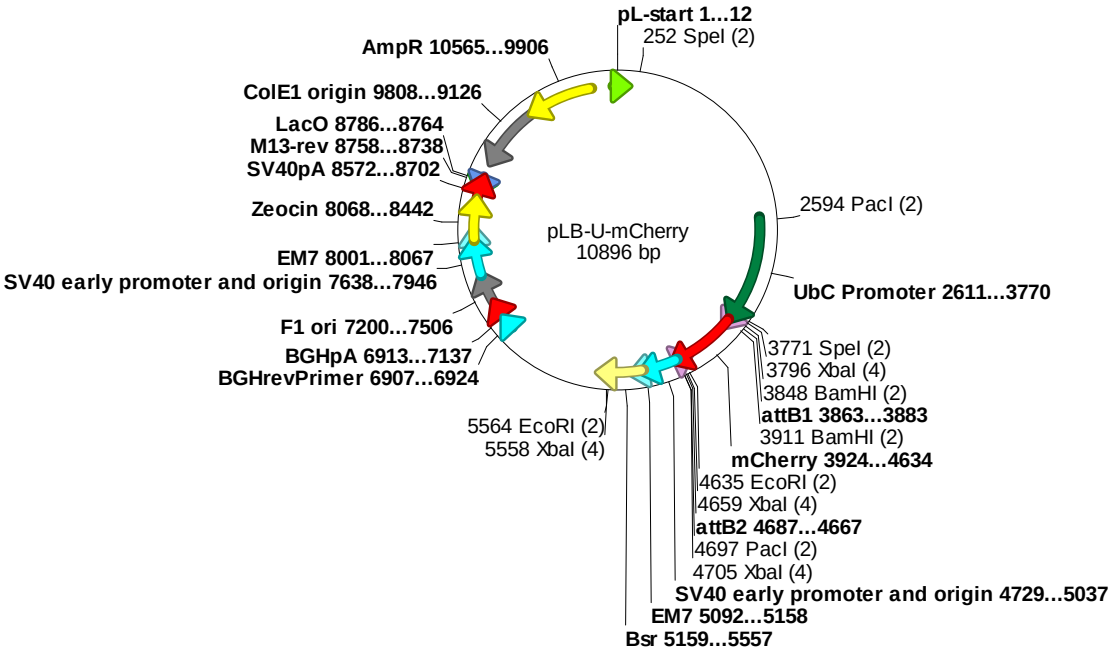

Supplement 2. Map of pLB-U-mKate2.

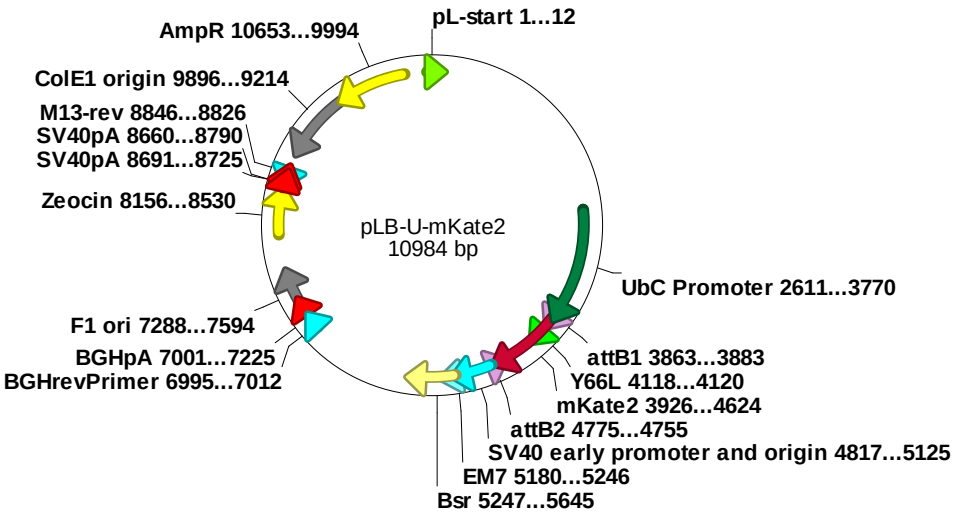

9.2 List of Figures

9.3 List of Tables

9.4 List of Abbreviations

AKT1	RAC-alpha serine/threonine-protein kinase
APC	antigen-presenting cell
APS	ammonium persulfate
BLI	bioluminescence imaging
Bp	base pair
BRAF	v-Raf murine sarcoma viral oncogene homolog B1
BSA	bovine serum albumin
bsAb	bispecific antibody
CD	cluster of differentiation
CDK4	cyclin-dependent kinase 4
CDKN2A	cyclin-dependent kinase inhibitor 2A
cDNA	complementary DNA
C_H1 domain	cysteine/histidine-rich 1 domain
CMV	Cytomegalovirus
CMV-IEPE	CMV immediate early promoter enhancer
CpG site	—C—phosphate—G—
CS-GAG	chondroitin sulfate glycosaminoglycan
CSPG4	chondroitin sulfate proteoglycan 4
CTD	C-terminal domain
CTL	cytotoxic T cell
CTLA-4	cytotoxic T-Lymphocyte Antigen 4
DFS	disease-free survival
DMEM	Dulbecco’s Modified Eagle’s Medium
Ham’s F-12	Nutrient Mixture F-12
DMSO	dimethyl sulfoxide
DNA	deoxyribonucleic acid
DPBS	Dulbecco`s Phosphate Buffered Saline
DTT	dithiothreitol
E.Coli	*Escherichia coli*
EDTA	ethylenediaminetetraacetic acid

ELISA	enzyme linked immunosorbent assay
EMT	epithelial-mesenchymale transition
ERK	extracellular-signal-regulated kinases
ES cells	embryonic stem cells
EtBr	ethidium bromide
FACS	fluorescent activated cell sorter
FAK	focal adhesion kinase
FBS	fetal bovine serum
FCS	fetal calf serum
FDA	Food and Drug Administration
FP	fluorescent protein
F_v	variable domain
gag	group-specific antigen
GBM	glioblastoma
GFP	green fluorescent protein
gp	glycoprotein
HCl	hydrochloric acid
HEK cells	human embryonic kidney cells
HeLa cells	Henrietta Lacks cells
HEPES	4-(2-hydroxyethyl)-1-piperazineethanesulfonic acid
HIV	human immunodeficiency virus
pLP1	proteolipid protein 1
pLP2	proteolipid protein 2
HLA	human leukocyte antigen
HMW-MAA	high molecular weight-melanoma associated antigen
HRP	horseradish peroxidase
IFN-α	interferon-alpha
Ig	immunoglobulin
PE	phycoerythrin
IKK	IκB kinase
IκB	inhibitor of kappa B
IL-2	interleukin 2

IL2Rγ	interleukin 2 receptor gamma-chain
IN	integrase
IVIS	In Vivo Imaging System
kDa	kilodalton
LB	lysogeny broth
LTR	long terminal repeat
LV	lentivirus
MAPK	mitogen-activated protein kinase
mEGFP	monomeric enhanced green fluorescent protein
MEM	Minimum Essential Medium
MeOH	methanol
MFI	mean fluorescence intensity
MITF	melanocyte lineage-specific transcription factor
MMP	matrix metalloproteinases
mRFP	monomeric red fluorescence protein
mRNA	messenger ribonucleic acid
Nef	negative factor
NFκB	nuclear factor 'kappa-light-chain-enhancer'
NG2	nerve/glial antigen 2
NK-cell	natural killer cell
NOD	non-obese diabetic
NSG	NOD.Cg-Prkdc^{scid} Il2rg^{tm1Wjl}/SzJ
OD	optical density
OS	overall survival
PBMC	peripheral blood mononuclear cell
pDNA	plasmid DNA
PET	positron emission tomography
PFS	progression-free survival
pH	power of hydrogen
PHA	phytohemagglutinin
PI3K	phosphoinositide 3-kinase
PIC	preintegration complex

PKCα	protein kinase C alpha
Pol	polymerase
Rev	regulator of virion expression
RFP	red fluorescence protein
RGP	radial growth phase
RNA	ribonucleic acid
RPMI 1640	Roswell Park Memorial Institute 1640
RSV	Rous sarcoma virus
RT	reverse transdcriptase
RTK	receptor tyrosine kinase
RT-PCR	reverse transcription polymerase chain reaction
RV	retrovirus
Sc	single-chain
sc-bsAb	single-chain bispecific antibody
scF_v	single-chain variable domain
Scid	severe combined immunodeficiency
SDS	sodium dodecyl sulfate
SH3 domain	SRC Homology 3 Domain
shRNAs	small hairpin RNA
SIN	self-inactivation
Sirpa	signal-regulatory protein alpha
Src	sarcoma
SV40	Simian virus 40
TAE	Tris-acetate-EDTA
Tat	trans-activator of transcription
TBS	Tris-Buffered Saline
TCR	T-cell receptor
TEMED	tetramethylethylenediamine
TMZ	Temozolomide
TP53	tumor protein p53
UbC	Ubiqutin C
UV	ultra-violet

VGP	vertical growth phase
V_H	heavy-chain V-region
vif	virion infectivity factor
V_L	light-chain V-region
Vpr	viral protein R
Vpu	viral protein U
VSV	Vesicular stomatitis virus
VSV-G	Vesicular stomatitis virus envelope glycoprotein
WPRE	Woodchuck Hepatitis Virus Posttranscriptional Regulatory Element
WST	Water soluble tetrazolium
X-ray	Röntgen radiation
YFP	yellow fluorescent protein
Ψ	packaging signal psi

9.5 Curriculum Vitae

Work experience

Since 05/2013: *Christian Doppler Laboratory for Chemical Analysis of Allergenic Food Contaminants*
University of Natural Resources and Life Sciences, Vienna
Department IFA-Tulln, 3430 Tulln
Student assistant (cell culture, antibody purification, ELISA, etc.)

02/2012-10/2012: *Christian Doppler Laboratory for Innovative Immunotherapy*
University of Veterinary Medicine, 1210 Vienna
Internship (2 months) and practical part of diploma thesis (cell culture, flow cytometry, Western blotting, etc.)

Since 05/2010: *Dr. Rainer Ullrich*
3423 St.Andrä-Wördern; Austria
Medical Secretary

08/2006-05/2010: *MR Dr. Robert Lindner*
1140 Vienna; Austria
Medical Secretary

Symposia

March 29th –
March 30th, 2012: *Zoonotische* Influenzaviren – Erreger zwischen Banalität und globaler Bedrohung. Vienna; Austria

Education

Since 2005:	*University of Vienna* Molecular Biology with specialization on Molecular Medicine, Microbiology/Immunology and Neuroscience
2000-2004:	*Bundesoberstufenrealgymnasium Krems* Secondary school with focus on natural sciences and mathematics

Skills

German (first language)
English (fluent)
Microsoft Office (Word, Excel, PowerPoint)